

Perturbative approach to time-dependent quantum systems and applications to one-crossing multistate Landau-Zener models

Rongyu Hu¹ and Chen Sun^{1,*}

¹*School of Physics and Electronics, Hunan University, Changsha 410082, China*

We formulate a perturbative approach for studying a class of multi-level time-dependent quantum systems with constant off-diagonal couplings and diabatic energies being odd functions of time. Applying this approach to a general multistate Landau-Zener (MLZ) model with all diabatic levels crossing at one point (named the one-crossing MLZ model), we derive analytical formulas of all its transition probabilities up to 4th order in the couplings. For one-crossing MLZ models it is difficult to obtain such analytical results by other kinds of approximation methods; thus, these perturbative results can serve as reliable benchmarks for future studies of any one-crossing MLZ models that have not been exactly solved.

I. INTRODUCTION

Finding exact analytical solutions to quantum systems with a time-dependent Hamiltonian is generally regarded as a difficult task. This remains true for a Hamiltonian with linear time-dependence — perhaps the simplest form of time-dependence. Such linearly time-dependent quantum models are known as the multistate Landau-Zener (MLZ) models since they are generalizations of the famous Landau-Zener (LZ) model [1–4] to systems with numbers of levels larger than 2. Although the LZ model can be exactly solved by different methods [5, 6] (meaning that all its transition probabilities for an evolution from $t = -\infty$ to $t = \infty$ can be expressed in analytical forms), exact solutions of MLZ models have been found only for models with special structures of their Hamiltonians [7–34]. Typical methods to exactly solve LZ or MLZ models include usages of special functions [2], Laplace transformations and contour integrations [3, 8, 10, 13], analytical constraints [23, 24], the unitary integration method [7, 11, 14–16], and the recently developed usage of integrability [25–34]. Besides, for MLZ models not exactly solvable, exact results for some of their transition probabilities may still be obtained [35–40].

When exact solutions are absent, one naturally turn to approximation methods or numerical simulations. For MLZ models, possible approximation approaches include the independent crossing approximation, the exact WKB approach, and the Dykhne formula. The independent crossing approximation, proposed in [35], states that when all crossings of pairs of levels are well-separated, a transition probability between two states can be approximated by adding contributions from all semiclassical paths connecting the two states, with each contribution being a product of successive pairwise transition probabilities along a path [41]. The exact WKB approach proves to be a powerful method to obtain approximate solutions both in the adiabatic [42] and in the diabatic [43, 44] regime. It also assumes all level crossings to be

pairwise. The Dykhne formula [45–47] predicts transition probabilities in the adiabatic regime, but its application to models with more than 2 levels is not always valid [48]. Numerical simulation of the Schrödinger equation is also a commonly-used method for MLZ problems [49, 50]. Numerical solutions can be useful in obtaining analytical expressions of transition probabilities by fitting [2], and possibly by symbolic regression algorithms [52]; especially, machine learning packages [53, 54] have been used to find analytical solutions to MLZ models recently [55].

Among MLZ models there is a special class consisting of models with all diabatic levels crossing at a single point; we will call this class the “*one-crossing MLZ model*” for brevity. Some physically important models belong to this class. For example, a nanomagnet with spin S under linearly-changing magnetic field is described by a one-crossing MLZ model with $2S + 1$ levels; such a system was realized in experiments on molecular clusters [56]. Another example is the driven Tavis-Cummings model [21, 22] — a basic model in quantum optics — which describes interaction between a bosonic mode and an arbitrary size spin under a linear sweep of magnetic field. Besides physical applications, one-crossing MLZ models are also of special theoretical importance, because they can be used as building blocks to construct more complex solvable systems if they themselves are solvable [26]. In [24], one-crossing MLZ models were studied in detail, and some models are exactly solved by using analytical constraints on the scattering matrices and symmetry properties. Exactly solvable one-crossing MLZ models can also be generated as degenerate limits of solvable MLZ models with parallel levels [12, 21]. The unitary integration method [7, 11, 14–16] is another powerful approach to exactly solve a one-crossing MLZ model whose Hamiltonian can be expressed in terms of generators of sufficiently simple Lie algebras. Still, all these methods require strict constraints on structures of Hamiltonians, and for most one-crossing MLZ models exact solvability seem not possible. As for approximation methods, the independent crossing approximation and the exact WKB method do not work for one-crossing MLZ models with more than two levels, since they assume that all cross-

* chensun@hnu.edu.cn

ings are pairwise. Therefore, one-crossing MLZ models require special treatment on their own.

In this paper, we obtain analytical results for one-crossing MLZ models at the diabatic limit. We first formulate a perturbative approach for treating a general time-dependent quantum system with constant off-diagonal couplings and diabatic energies being odd functions of time. We then apply this approach to one-crossing MLZ models and derive analytical expressions of all the transition probabilities up to 4th order in the couplings, which become asymptotically exact at the diabatic limit. These results of probabilities are general in the sense that they work for *any* one-crossing MLZ models, exactly solvable or not.

Our work is expected to contribute to theoretical studies of time-dependent quantum problems in two ways. First, our results for one-crossing MLZ models should be valuable for any models not exactly solved — as discussed previously, such analytical results for one-crossing MLZ models seem not achievable by other approximation methods. Second, the general perturbative approach has its own value — it may be applied to other multistate time-dependent quantum models with more general forms of time-dependence instead of linear time-dependence.

This paper is organized as follows. In Section II, we formulate the general perturbative approach that expresses the transition probabilities as power series of the couplings. Section III is devoted to applications of the approach to one-crossing MLZ models (with technical calculation details giving in the supplemental material); in particular, transition probabilities up to 4th order in the couplings are obtained in analytical forms (see Eqs. (37)–(41)), and interpretation of these results are discussed. Section IV applies the results in Section III to specific MLZ models, especially models which have not been exactly solved. Finally, in Section V we present conclusions and discussions.

II. GENERAL PERTURBATIVE APPROACH

We consider an N -state quantum system evolving under the Schrödinger equation with a real symmetric time-dependent Hamiltonian $H(t)$ (with \hbar setting to 1):

$$i\frac{d\psi}{dt} = H(t)\psi, \quad H(t) = E(t) + gA, \quad (1)$$

where $E(t) = \text{diag}(\varepsilon_1(t), \varepsilon_2(t), \dots, \varepsilon_N(t))$ is a diagonal matrix, A is an off-diagonal matrix (namely, a matrix with all diagonal elements being zero) that does not depend on time, and g is a real number which we will take as the parameter of perturbation expansion. The eigenvalues of the matrix $E(t)$, namely the functions $\varepsilon_j(t)$, are called *diabatic energies* or *diabatic levels*, and the eigenstates of $E(t)$ are called *diabatic states*. We will assume that every $\varepsilon_j(t)$ is odd in time, namely, the matrix $E(t)$ is odd: $E(-t) = -E(t)$. Specifically, any one-crossing

MLZ model, which we will focus on later, satisfies this property. The element A_{jk} characterizes the interaction strength between diabatic states j and k ; we call it the *coupling* between the two states.

A note on the units used throughout this paper is in order. We set \hbar to 1 and time t to be dimensionless, so energy is also dimensionless. gA_{jk} as a whole has units of energy, and we take both g and A_{jk} to be dimensionless. Therefore, no explicit units will appear throughout the text.

Let's consider the evolution operator between symmetric times $-t$ and t :

$$S(t) \equiv U(t, -t) = \mathcal{T}e^{-i \int_{-t}^t H(s)ds}, \quad (2)$$

where \mathcal{T} is the time-ordering operator. Denote the transition probability corresponding to this evolution from a diabatic state k to a diabatic state j as $P_{jk}(t)$ (note the order of the indices in $P_{jk}(t)$). $P_{jk}(t)$ is connected to the elements of $S(t)$ by $P_{jk}(t) = |S_{jk}(t)|^2$. In the limit $t \rightarrow \infty$, i.e. when the evolution is from infinite past to infinite future, if the differences between any diabatic energies $\varepsilon_j(t)$ goes to infinity, then the transition probabilities should approach constants: $P_{jk}(t \rightarrow \infty) = P_{jk}$. We are especially interested in these transition probabilities at infinite times. As discussed in the introduction, for a general model it is usually difficult to obtain analytical expressions of P_{jk} .

A. Perturbative approach

We now formulate a perturbative approach for the model (1) to express the transition probabilities $P_{jk}(t)$ as power series expansions of the parameter g around $g = 0$, namely, expansions at the diabatic limit [57]. Our approach is a generalization of Waxman's perturbative approach on 2-state models [58] to multistate systems.

The approach starts from differentiating (2) over t :

$$i\partial_t S(t) = H(t)S(t) + S(t)H(-t). \quad (3)$$

Plugging in $H(t) = E(t) + gA$ and $H(-t) = -E(t) + gA$ (recall that $E(-t) = -E(t)$), we get

$$i\partial_t S(t) = [E(t), S(t)] + g\{A, S(t)\}, \quad (4)$$

where “[,]” and “{,}” denote commutators and anti-commutators, respectively. Let's define a diagonal matrix

$$\Phi(t) = \int_0^t E(s)ds = \text{diag}(\phi_1(t), \dots, \phi_N(t)) \quad (5)$$

where we denoted

$$\phi_j(t) = \int_0^t ds \varepsilon_j(s) \quad (6)$$

with $j = 1, 2, \dots, N$. Namely, $\phi_j(s)$ is a phase accumulated by the diabatic energy $\varepsilon_j(s)$ in the time interval

$(0, t)$. Following [58], we perform a unitary transformation from $S(t)$ to an auxiliary operator $W(t)$ by:

$$S(t) = e^{-i\Phi(t)} W(t) e^{i\Phi(t)}. \quad (7)$$

This transformation does not change the modulus of each component of the matrix, so $P_{ij}(t) = |W_{ij}(t)|^2$. Plugging (7) into the differential equation (4) gives a differential equation for $W(t)$ in which the commutator term is eliminated:

$$i\partial_t W(t) = g\{\tilde{A}(t), W(t)\}, \quad (8)$$

where for notation simplicity we defined

$$\tilde{A}(t) = e^{i\Phi(t)} A e^{-i\Phi(t)}. \quad (9)$$

Note that $\tilde{A}(t)$ is Hermitian by construction. Its elements are given by

$$\begin{aligned} \tilde{A}_{jj}(t) &= 0, \\ \tilde{A}_{jk}(t) &= e^{i(\phi_j(t) - \phi_k(t))} A_{jk}, \quad \text{for } j \neq k. \end{aligned} \quad (10)$$

Integrating both sides of (8) with respect to t and noticing that $W(0) = 1$ (for simplicity, we use 1 to denote an $N \times N$ identity matrix here and later on) then gives

$$W(t) = 1 - ig \int_0^t ds \{\tilde{A}(s), W(s)\}. \quad (11)$$

This integral equation (11) can be solved perturbatively in orders of g . Let's write $W(t)$ as Taylor series expansion of g :

$$W(t) = \sum_{n=0}^{\infty} W_n(t) g^n. \quad (12)$$

Plugging it into (11), we get

$$\sum_{n=0}^{\infty} W_n(t) g^n = 1 - ig \int_0^t ds \{\tilde{A}(s), \sum_{n=0}^{\infty} W_n(s) g^n\}. \quad (13)$$

On the two sides of this equation the coefficients at each order of g should equal. This gives $W_0(t) = 1$ and a recursion relation

$$W_{n+1}(t) = -i \int_0^t ds \{\tilde{A}(s), W_n(s)\}, \quad (14)$$

where $n = 0, 1, 2, \dots$. Thus, $W_n(t)$ can be obtained iteratively. $W_1(t)$ reads

$$W_1(t) = -2i \int_0^t ds \tilde{A}(s), \quad (15)$$

and $W_n(t)$ for $n \geq 2$ can be expressed in terms of multiple integrals:

$$\begin{aligned} W_n(t) &= 2(-i)^n \int_0^t ds_1 \int_0^{s_1} ds_2 \dots \int_0^{s_{n-1}} ds_n \\ &\{\tilde{A}(s_1), \{\tilde{A}(s_2), \dots \{\tilde{A}(s_{n-1}), \tilde{A}(s_n)\} \dots \}\}. \end{aligned} \quad (16)$$

$W_2(t)$ can be simplified using symmetry. Since $\{\tilde{A}(s_1), \tilde{A}(s_2)\}$ is symmetric in s_1 and s_2 , a change of the region of the double integral from the triangle $0 < s_2 < s_1 < t$ to a square $0 < s_1, s_2 < t$ would simply double the integral, so

$$W_2(t) = -2 \left[\int_0^t ds \tilde{A}(s) \right]^2. \quad (17)$$

Thus, $W_1(t)$ and $W_2(t)$ involve only evaluation of a single integral $\int_0^t ds \tilde{A}(s)$. One may wonder if the same is true for a general $W_n(t)$, but it turns out starting from $W_3(t)$ one would have to perform multiple integrals. $W_3(t)$ reads:

$$W_3(t) = 2i \int_0^t ds_1 \int_0^{s_1} ds_2 \int_0^{s_2} ds_3 \{\tilde{A}(s_1), \{\tilde{A}(s_2), \tilde{A}(s_3)\}\}. \quad (18)$$

Since $\{\tilde{A}(s_1), \{\tilde{A}(s_2), \tilde{A}(s_3)\}\}$ is not completely symmetric in s_1, s_2 and s_3 (the terms $\tilde{A}(s_2)\tilde{A}(s_1)\tilde{A}(s_3)$ and $\tilde{A}(s_3)\tilde{A}(s_1)\tilde{A}(s_2)$ are missing), the above replacement of integral region cannot be performed. If we add and subtract the two missing terms, $W_3(t)$ is rewritten into a more symmetric form:

$$\begin{aligned} W_3(t) &= 2i \left[\int_0^t ds \tilde{A}(s) \right]^3 \\ &- 2i \int_0^t ds \left[\int_0^s ds_1 \tilde{A}(s_1) \right] \tilde{A}(s) \left[\int_0^s ds_1 \tilde{A}(s_1) \right]. \end{aligned} \quad (19)$$

The first term arises from the completely symmetric combination and involve only $\int_0^t ds \tilde{A}(s)$, whereas the second term involves a multiple integral that cannot be simplified. $W_n(t)$ for $n > 3$ involve multiple integrals in more complicated forms.

Let's denote the matrix elements of $W_n(t)$ as $W_{n,jk}(t)$. In terms of $W_{n,jk}(t)$, the transition probabilities $P_{jk}(t)$ can be expressed as series expansions of g :

$$P_{jk}(t) = \left| \sum_{n=0}^{\infty} W_{n,jk}(t) g^n \right|^2 = \sum_{n=0}^{\infty} P_{n,jk}(t) g^n, \quad (20)$$

where

$$P_{n,jk}(t) = \sum_{m=0}^n W_{m,jk}(t) W_{n-m,jk}^*(t). \quad (21)$$

Thus, the expansion coefficient $P_{n,jk}(t)$ is determined by all $W_{m,jk}(t)$ with $m \leq n$. Taking the $t \rightarrow \infty$ limit, we get series expansions for probabilities at infinite times:

$$P_{jk} \equiv \lim_{t \rightarrow \infty} P_{jk}(t) = \sum_{n=0}^{\infty} P_{n,jk} g^n, \quad (22)$$

where we defined

$$P_{n,jk} \equiv \lim_{t \rightarrow \infty} P_{n,jk}(t). \quad (23)$$

We will denote the matrix formed by $P_{n,jk}(t)$ as $P_n(t)$, and its limit at $t \rightarrow \infty$ simply by P_n .

We end this subsection by a remark on a different perturbative approach. We started from considering an evolution operator $S(t) \equiv U(t, -t)$ between symmetric times (see Eq. (2)). One could also take a different perturbative approach by considering an evolution between nonsymmetric times, namely $U(t_2, t_1)$, and finally take $t_1 \rightarrow -\infty$ and $t_2 \rightarrow \infty$. The intermediate procedures in such a approach will be different, but we expect that it will give the same final results for the probabilities at infinite times (i.e. P_{jk}) as the current approach, namely,

$$\lim_{t_1 \rightarrow -\infty, t_2 \rightarrow \infty} |U_{jk}(t_2, t_1)|^2 = \lim_{t \rightarrow \infty} |U_{jk}(t, -t)|^2 = P_{jk}. \quad (24)$$

One can understand this as follows. In a sense, the two limits correspond to the ordinary value and the Cauchy principal value of an infinite integral from $-\infty$ to ∞ , respectively. If the two limits both exist, they must equal, since the second limit is a special case of the first limit (in other words, if they do not equal, the first limit should not exist at all).

Before considering MLZ models, we discuss some properties of $P_n(t)$ for a general model (1). All properties discussed in the following two subsections hold at any t , so they hold especially in the limit $t \rightarrow \infty$. They will be useful when considering MLZ models in the next section.

B. Structure in terms of connectivity graphs

We first make an interesting observation on an intuitive structure of the matrix elements of $W_n(t)$ in (16), and further of $P_{n,jk}(t)$ in (21).

For this purpose, we introduce the notation of a *connectivity graph*: given any N -state model (1), we associate to its Hamiltonian a graph (in the graph-theoretical sense), with each vertex labelled by j corresponding to a diabatic level j , and each edge corresponding to a *non-zero* coupling A_{jk} between a pair of levels j and k . Such a graph illustrates how the levels are connected by couplings, hence the name “connectivity graph”. For example, Fig. 1 shows a connectivity graph for a 5-state model.

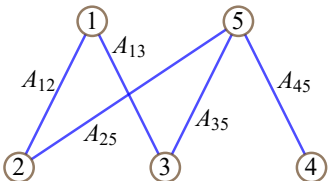


FIG. 1. The connectivity graph for a 5-state model with non-zero couplings A_{12} , A_{13} , A_{25} , A_{35} , and A_{45} .

It turns out that connectivity graphs are helpful in understanding the structure of the elements $W_{n,jk}(t)$ of the

matrix $W_n(t)$ in (16). Despite the appearance of multiple integrals and anti-commutators, we observe that dependence of $W_{n,jk}(t)$ on the couplings is actually of a simple form. This observation follows simply from the definition of matrix products. Consider for example a product of three matrices X , Y and Z , its matrix elements is given by a summation $(XYZ)_{jk} = \sum_{l,m} X_{jl} Y_{lm} Z_{mk}$. Similarly, we can write $W_{n,jk}(t)$ as such a summation, and note that for each term in this summation there are always n factors of the couplings A_{lm} which do not depend on time and thus can be “pulled out of” the integrals (recall the definition of \bar{A}_{jk} in (10)). Therefore, $W_{n,jk}(t)$ must take the following form

$$W_{n,jk}(t) = \sum_{l_1, l_2, \dots, l_{n-1}} I_{l_1 l_2 \dots l_{n-1}} A_{jl_1} A_{l_1 l_2} \dots A_{l_{n-1} k}, \quad (25)$$

where the sum is taken over all possible choices of $1 \leq l_1, l_2, \dots, l_{n-1} \leq N$, and $I_{l_1 l_2 \dots l_{n-1}}$ involves n -dimensional multiple integrals that depend on the diabatic energies but not on the couplings. Now note that if any factor in a certain product $A_{jl_1} A_{l_1 l_2} \dots A_{l_{n-1} k}$ is zero, then contribution of this product to the sum (25) vanishes. Thus, every different term in (25) corresponds to a different length- n path from the vertex j to the vertex k in the connectivity graph. By identifying each length- n path in the connectivity graph, one can readily read off the structure of $W_{n,jk}(t)$. For example, in the connectivity graph in Fig. 1, let’s identify the structure of $W_{n,12}(t)$ for $n = 1, 2, 3$. For $n = 1$, there is one length-1 path $1 \rightarrow 2$, corresponding to a single contribution to $W_{1,12}(t)$ proportional to A_{12} . For $n = 2$, there is no length-2 path, so we know immediately that $W_{2,12}(t) = 0$. For $n = 3$, there are four length-3 paths: $1 \rightarrow 2 \rightarrow 1 \rightarrow 2$, $1 \rightarrow 2 \rightarrow 5 \rightarrow 2$, $1 \rightarrow 3 \rightarrow 1 \rightarrow 2$ and $1 \rightarrow 3 \rightarrow 5 \rightarrow 2$ (note that the paths do not need to be self-avoiding), each corresponding to a contribution to $W_{3,12}(t)$ proportional to A_{12}^3 , $A_{12}A_{25}^2$, $A_{12}A_{13}^2$, and $A_{13}A_{35}A_{25}$, respectively (note that $A_{lm} = A_{ml}$).

The above structure of $W_{n,jk}(t)$ in turn determines the structure of $P_{n,jk}(t)$ via (21). Since $P_{n,jk}(t)$ is written as a sum of $W_{m,jk}(t)W_{n-m,jk}^*(t)$, every different pair of paths from j to k with lengths m and $n - m$ (where m ranges from 1 to $n - 1$) in the connectivity graph contributes a term in $P_{n,jk}(t)$. Equivalently, every different length- n cycle that passes the vertices j and k corresponds to a contribution to $P_{n,jk}(t)$. For example, in the connectivity graph in Fig. 1, to read off the form of $P_{4,12}(t)$, note that there are 4 distinct length-4 cycles that passes vertices 1 and 2: $1 \rightarrow 2 \rightarrow 1 \rightarrow 2 \rightarrow 1$, $1 \rightarrow 2 \rightarrow 5 \rightarrow 2 \rightarrow 1$, $1 \rightarrow 3 \rightarrow 1 \rightarrow 2 \rightarrow 1$ and $1 \rightarrow 3 \rightarrow 5 \rightarrow 2 \rightarrow 1$ (again the cycles do not need to be self-avoiding), each corresponding to a contribution to $P_{4,12}(t)$:

$$P_{4,12}(t) = c_1 A_{12}^4 + c_2 A_{12}^2 A_{25}^2 + c_3 A_{12}^2 A_{13}^2 + c_4 A_{12} A_{13} A_{35} A_{25}, \quad (26)$$

where c_1 to c_4 are coefficients which do not depend on any couplings A_{lm} .

This interpretation of $P_{n,jk}(t)$ on connectivity graphs will be useful in later sections when we deal with MLZ models. Here we mention one of its direct consequences — if two diabatic levels j and k are not directly coupled (i.e. $A_{jk} = 0$), then $P_{n,jk}(t)$ for $n \leq 3$ all vanish, and the leading order contribution to $P_{jk}(t)$ is at least of the 4th order in g (we write this briefly as $P_{jk}(t) = O(g^4)$). More generally, if the shortest path(s) between two vertices j and k in the connectivity graph contains d edges (namely, the “distance” between the two levels is d), then $P_{n,jk}(t)$ for $n \leq 2d - 1$ all vanish, and $P_{jk}(t) = O(g^{2d})$. For example, in Fig. 1 the distance between vertices 1 and 5 is 2, so $P_{15}(t) = O(g^4)$; the distance between vertices 1 and 4 is 3, so $P_{14}(t) = O(g^6)$.

C. Symmetry properties

Besides the interpretation in terms of connectivity graphs, $P_n(t)$ also have some symmetry properties. They follow directly from an interesting observation on $W_n(t)$. Taking Hermitian conjugate of the recursion relation (14) and using the fact that $\tilde{A}(s)$ is Hermitian gives:

$$W_{n+1}^\dagger(t) = i \int_0^t ds \{ \tilde{A}(s), W_n^\dagger(s) \}. \quad (27)$$

Since $W_0(t) = 1$ is Hermitian, we obtain

$$W_n^\dagger(t) = W_n(t), \quad \text{for } n \in \text{even}, \quad (28)$$

$$W_n^\dagger(t) = -W_n(t), \quad \text{for } n \in \text{odd}. \quad (29)$$

namely, $W_n(t)$ is Hermitian/anti-Hermitian for even/odd n .

Several properties of $P_n(t)$ follows. Using (21), for $P_n(t)$ with an even n ,

$$P_{n,kj}(t) = \sum_{m=0}^n W_{m,kj}(t) W_{n-m,kj}^*(t) = P_{n,jk}(t), \quad (30)$$

and for $P_n(t)$ with an odd n ,

$$P_{n,kj}(t) = \sum_{m=0}^n W_{m,kj}(t) W_{n-m,kj}^*(t) = -P_{n,jk}(t). \quad (31)$$

Namely, the matrix $P_n(t)$ is symmetric/anti-symmetric for even/odd n . Therefore, evaluation of $P_{n,jk}(t)$ for all $j \leq k$ is sufficient to determine the whole matrix $P_n(t)$.

A direct consequence of (31) is that

$$P_{n,jj}(t) = 0, \quad \text{for } n \in \text{odd}, \quad (32)$$

namely, the diagonal elements of $P(t)$ can only contain terms of even orders in g . In other words, $P_{jj}(t)$ must take a form:

$$P_{jj}(t) = 1 + P_{2,jj}(t)g^2 + P_{4,jj}(t)g^4 + \dots \quad (33)$$

The off-diagonal elements of $P(t)$ also possess certain properties. First, since $W_0(t) = 1$ one has $W_{0,jk}(t) = 0$ for $j \neq k$, and it follows directly from (20) that the leading non-vanishing term of P_{jk} must be at least of 2nd order in g :

$$P_{jk}(t) = P_{2,jk}(t)g^2 + P_{3,jk}(t)g^3 + \dots, \quad \text{for } j \neq k. \quad (34)$$

Second, note that $P(t)$, as a matrix of probabilities, is doubly stochastic; especially $P_{jk}(t)$ at any g cannot be negative. Let's denote the leading non-vanishing order of $P_{jk}(t)$ as n_l (excluding the extremal case that $P_{jk}(t)$ is identically zero). If n_l is an odd number, then at sufficiently small g either $P_{n_l,jk}(t)$ or $P_{n_l,kj}(t)$ is negative, which violates the doubly stochastic property. So n_l must be even — the leading non-vanishing term of $P_{jk}(t)$ must be of an even order in g .

III. APPLICATIONS TO MULTISTATE LANDAU-ZENER MODEL

The perturbative approach described in the Section II works for a general quantum system of the form (1). In this paper, we focus on its application to MLZ models, namely, models whose matrix $E(t)$ is linear in t . Since the diabatic energies are assumed to be odd, $E(t)$ must take the form:

$$E(t) = \text{diag}(b_1 t, b_2 t, \dots, b_N t). \quad (35)$$

The parameters b_j are called *slopes*; we take all of them to be different and assume without loss of generality that $b_1 > b_2 > \dots > b_N$. This model is a one-crossing MLZ model with the crossing of levels at the point $(t, E) = (0, 0)$, and its diabatic energy diagram shown in Fig. 2. Note that any other one-crossing MLZ model crossing at another point $(t, E) \neq (0, 0)$ can be transformed to this model by a shift of t and E without changing the probabilities. Thus, the model (1) with $E(t)$ given by (35) actually presents the most general form of a one-crossing MLZ model.

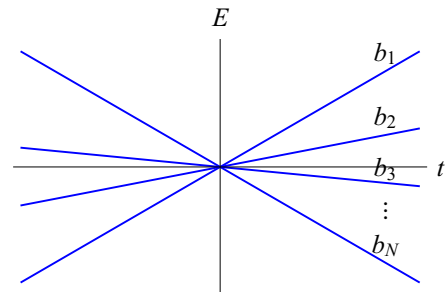


FIG. 2. Diabatic energy diagram of a one-crossing MLZ model with slopes $b_1 > b_2 > \dots > b_N$.

In this section, we will present results of transition probabilities for this general one-crossing MLZ model up

to 4th order in the couplings. We then explain these results via the connectivity graph interpretation discussed in Section IIB. We also discuss several special cases of the initial and final levels j and k , and a specific class of model where the general results of probabilities reduce to simpler forms, in order to provide further physical intuition of the results.

A. Results of transition probabilities up to g^4

By using the perturbative approach in Section IIA, in particular (16) and (21), we calculated explicitly the matrix elements of P_n for this general one-crossing MLZ model up to $n = 4$, namely, transition probabilities up to 4th order in the couplings. These calculations (especially those for the 4th order contributions) are technical and tedious so their details are put into the supplemental material, and here we present directly the results.

Let's define the combinations

$$\lambda_{jk} = \sqrt{\frac{\pi}{|b_{jk}|}} A_{jk}, \quad \text{for } j \neq k. \quad (36)$$

In terms of these λ_{jk} , the probabilities P_{jk} with $j < k$ read:

$$P_{jk} = P_{2,jk}g^2 + P_{3,jk}g^3 + P_{4,jk}g^4 + O(g^5), \quad (37)$$

where

$$\begin{aligned} P_{2,jk} &= 2\lambda_{jk}^2, \\ P_{3,jk} &= 2\lambda_{jk} \left(\sum_l^{j < l < k} \lambda_{jl}\lambda_{lk} - \sum_l^{l < j \text{ or } l > k} \lambda_{jl}\lambda_{lk} \right), \\ P_{4,jk} &= \left(\sum_l^{l < j \text{ or } l > k} \lambda_{jl}\lambda_{lk} \right)^2 + \left(\sum_l^{j < l < k} \lambda_{jl}\lambda_{lk} \right)^2 \\ &\quad - \lambda_{jk}^2 \left(\sum_l^{l \leq k} \lambda_{jl}^2 + 3 \sum_l^{l > k} \lambda_{jl}^2 + \sum_l^{l \geq j} \lambda_{lk}^2 + 3 \sum_l^{l < j} \lambda_{lk}^2 \right) \\ &\quad - 2\lambda_{jk} \left(2 \sum_{l,p}^{p < j < l < k \text{ or } j < p < k < l} - \sum_{l,p}^{j < p < l < k} \right. \\ &\quad \left. + \sum_{l,p}^{j < l < k < p, l < j < p < k \text{ or } p < j < k < l} \right) \lambda_{jl}\lambda_{lp}\lambda_{pk}. \end{aligned} \quad (38)$$

All other probabilities are then determined by symmetry properties and the doubly stochastic property. According to the symmetry properties (30) and (31), the probabilities P_{jk} with $j > k$ is connected to those with $j < k$ by:

$$P_{jk} = P_{2,kj}g^2 - P_{3,kj}g^3 + P_{4,kj}g^4 + O(g^5). \quad (39)$$

The diagonal probabilities are given by $P_{jj} = 1 - \sum_{k \neq j} P_{jk}$. In particular,

$$P_{jj} = 1 + P_{2,jj}g^2 + P_{4,jj}g^4 + O(g^6), \quad (40)$$

where

$$P_{2,jj} = -2 \sum_k^{k \neq j} \lambda_{jk}^2, \quad P_{4,jj} = - \sum_k^{k \neq j} P_{4,jk}. \quad (41)$$

Therefore, the probabilities up to 4th order in the couplings can be expressed as polynomials of λ_{jk} with integer coefficients.

B. Interpretation of the results via connectivity graphs

The results (38), in particular the expression of the 4th order term $P_{4,jk}$, look complicated; but we note that each term in those expressions can be understood in terms of paths on connectivity graphs discussed in Section IIB; in this subsection we discuss this interpretation.

First, the form of the 2nd order contribution $P_{2,jk}$ can be directly read-off by considering length-1 paths from the states j to k (recall that λ_{jk} defined as (36) is proportional to A_{jk}). Of course there is only one such length-1 path if $A_{jk} \neq 0$; we denote this path as $j \rightarrow k$. This same path appears in $W_{1,jk}(t)$ and in $W_{1,jk}^*(t)$, so there is a single term in $P_{2,jk}$ which is proportional to A_{jk}^2 . Detailed calculations in the supplemental material show that the coefficients in front of A_{jk}^2 is $2\pi/|b_{jk}|$, which, upon defining λ_{jk} , then leads to the expression $2\lambda_{jk}^2$ for $P_{2,jk}$ in (38).

Second, let's consider the 3rd order contribution $P_{3,jk}$. Now we should identify one length-1 path and one length-2 path from the states j to k . The length-1 paths, like before, have only one possibility: $j \rightarrow k$. For length-2 paths, there can be $j \rightarrow l \rightarrow k$ where l can take any index except j and k . Thus, the result would be a sum of the form $P_{3,jk} = 2A_{jk} \sum_l A_{jl}A_{lk}c_l$, where c_l are coefficients independent of the couplings. Determining these coefficients by calculations, one obtains the result of $P_{3,jk}$ in (38). The coefficients for contributions from $j < l < k$ and from $l < j$ or $l > k$ turn out to be differ by a sign, so the expression of $P_{3,jk}$ in (38) contains two sums.

Finally, the complicated-look expression of the 4th order contribution $P_{4,jk}$ can be understood in the same manner. Possible contributions to $P_{4,jk}$ can arise in two ways: two length-2 paths, or a length-1 path and a length-3 path. Possibilities of length-1 and length-2 paths are discussed before. A length-3 path $j \rightarrow l \rightarrow p \rightarrow k$ should involve double summation of two indices l and p . We identify that the first line of $P_{4,jk}$ in (38) corresponds to contributions from two length-2 paths $j \rightarrow l \rightarrow k$ to $P_{4,jk}$, whereas the last three lines of $P_{4,jk}$ in (38) correspond to contributions from a length-1 path $j \rightarrow k$ and a length-3 path $j \rightarrow l \rightarrow p \rightarrow k$ to $P_{4,jk}$. Specifically, the second line of $P_{4,jk}$ corresponds to contributions where the length-3 path is self-intersecting, i.e. when $l = k$ or $p = j$. It turns out by detailed calculations that self-intersecting and self-avoided paths have coefficients of different forms, and the order of j, l, p, k also influences

the coefficients, leading to the various inequality conditions of the summations.

C. Transition probabilities between special levels

Now let's consider transitions between special levels where the result (38) reduces to simpler forms.

Case 1: A transition between the two levels with extremal slopes, i.e. with $j = 1$ and $k = N$. In this case, any other level l satisfies $j < l < k$, so certain sums in (38) vanish, leading to

$$\begin{aligned} P_{2,1N} &= 2\lambda_{1N}^2, \\ P_{3,1N} &= 2\lambda_{1N} \sum_l \lambda_{1l} \lambda_{lN}, \\ P_{4,1N} &= \left(\sum_l \lambda_{1l} \lambda_{lN} \right)^2 - \lambda_{1N}^2 \left(\sum_l \lambda_{1l}^2 + \sum_l \lambda_{lN}^2 \right) \\ &+ 2\lambda_{1N} \sum_{l,p}^{p < l} \lambda_{1l} \lambda_{lp} \lambda_{pN}, \end{aligned} \quad (42)$$

where the sums with no specified ranges should be understood as over all possible l .

Case 2: transitions between adjacent levels, i.e. with $k = j + 1$. Eq. (38) now reduces to:

$$\begin{aligned} P_{2,jk} &= 2\lambda_{jk}^2, \\ P_{3,jk} &= -2\lambda_{jk} \sum_l \lambda_{jl} \lambda_{lk}, \\ P_{4,jk} &= \left(\sum_l \lambda_{jl} \lambda_{lk} \right)^2 - 2\lambda_{jk} \sum_{l,p}^{p < j < k < l} \lambda_{jl} \lambda_{lp} \lambda_{pk} \\ &- \lambda_{jk}^2 \left(\sum_l^{l \leq k} \lambda_{jl}^2 + 3 \sum_l^{l > k} \lambda_{jl}^2 + \sum_l^{l \geq j} \lambda_{lk}^2 + 3 \sum_l^{l < j} \lambda_{lk}^2 \right), \end{aligned} \quad (43)$$

where again the sums with no specified ranges are over all possible l , and k should be understood as $j + 1$.

D. A specific class — the chain model

To provide more insight as well as illustrate how the connectivity graph interpretation described in Section IIIB works in more specific examples, in this subsection we consider in details a specific class of one-crossing MLZ models called the chain model, where the perturbative results of probabilities reduce to very simple forms.

This model has a coupling matrix A with all couplings being zero except between adjacent levels: $A_{jk} = 0 \forall$

$|j - k| > 1$. Its Hamiltonian is:

$$H = \begin{pmatrix} b_1 t & gA_{12} & 0 & \cdots & 0 & 0 \\ gA_{12} & b_2 t & gA_{23} & \cdots & 0 & 0 \\ 0 & gA_{23} & b_3 t & \cdots & 0 & 0 \\ \vdots & \vdots & \vdots & \ddots & \vdots & \vdots \\ 0 & 0 & 0 & \cdots & b_{N-1} t & gA_{N-1,N} \\ 0 & 0 & 0 & \cdots & gA_{N-1,N} & b_N t \end{pmatrix}. \quad (44)$$

Since only couplings between adjacent levels are finite, the associated connectivity graph is a chain connecting vertices $1, 2, \dots, N$ successively, as shown in Fig 3. Exact solution of a general chain model is not known. Below we write out perturbative results for this chain model according to Eq. (38) and with the help of the connectivity graph interpretation.



FIG. 3. The connectivity graph for an N -state chain model associated to the Hamiltonian (44).

We first consider transitions between adjacent levels. For a transition from level $k = 2$ to level $j = 1$, we see that there are one length-1 path $1 \rightarrow 2$, no length-2 paths, and two length-3 paths $1 \rightarrow 2 \rightarrow 1 \rightarrow 2$ and $1 \rightarrow 2 \rightarrow 3 \rightarrow 2$. The transition probability is then

$$P_{12} = P_{2,12}g^2 + P_{4,12}g^4 + O(g^5), \quad (45)$$

where

$$\begin{aligned} P_{2,12} &= 2\lambda_{12}^2, \\ P_{4,12} &= -\lambda_{12}^2 (2\lambda_{12}^2 + \lambda_{23}^2). \end{aligned} \quad (46)$$

(Note that although the forms of products of λ 's can be read off on the connectivity graph, we still need Eq. (38) to determine the coefficients in front of those products.) For a transition from level $k = j + 1$ to level j with $j > 1$ and $j + 1 < N$, we see that there are one length-1 path $j \rightarrow j + 1$, no length-2 paths, and three length-3 paths $j \rightarrow j + 1 \rightarrow j \rightarrow j + 1$, $j \rightarrow j - 1 \rightarrow j \rightarrow j + 1$, and $j \rightarrow j + 1 \rightarrow j + 2 \rightarrow j + 1$. Thus,

$$P_{j,j+1} = P_{2,j,j+1}g^2 + P_{4,j,j+1}g^4 + O(g^5), \quad (47)$$

where

$$\begin{aligned} P_{2,j,j+1} &= 2\lambda_{j,j+1}^2, \\ P_{4,j,j+1} &= -\lambda_{j,j+1}^2 (2\lambda_{j,j+1}^2 + \lambda_{j-1,j}^2 + \lambda_{j+1,j+2}^2). \end{aligned} \quad (48)$$

The transition probability $P_{N-1,N}$ from level N to level $N - 1$ is analogous to P_{12} , which we do not write out explicitly.

We then consider transitions between next-nearest levels, namely, from level $k = j + 2$ to level j . Now there is no length-1 path and one length-2 path $j \rightarrow j+1 \rightarrow j+2$. So the contribution up to 3rd order all vanish (see the end of Section IIB):

$$P_{j,j+2} = P_{4,j,j+2}g^4 + O(g^5), \quad (49)$$

and the 4th order contribution is of a simple form

$$P_{4,j,j+2} = \lambda_{j,j+1}^2 \lambda_{j+1,j+2}^2. \quad (50)$$

Finally, for a transition from level k to level j with $k - j > 2$, according to the properties described at the end of Section IIB, the leading order of $P_{j,k}$ is at least $2(k - j)$, namely, $P_{j,k} = O(g^{2(k-j)})$.

These results apply to a general chain with arbitrary number of states N . At the end of Section IVB, we are going to compare these perturbative results to numerical results for a 6-state chain model.

IV. EXAMPLES

In this section, we apply the results of probabilities of one-crossing MLZ models, i.e. Eqs. (37)-(41), to more specific models. We first discuss a few models which are exactly solvable. For these models a perturbative approach is actually not necessary, but their exact solutions can serve as tests of our perturbative results. We then consider several models whose exact solutions have not been found. We expect such models to be the arenas where our perturbative results can play important roles because, as discussed in the introduction, such analytical results are difficult to be obtained by other kinds of approximation methods. For example, the 3-state model to be discussed in Section IVB1 describes the diabatic dynamics of a spin-1 nanomagnet under a fast linear sweep of magnetic field, which can guide experiments e.g. on molecular clusters [56].

Note that although we considered g as the parameter of perturbative expansion, g can actually be absorbed into the couplings A_{jk} , after which the expansions can be viewed as on the couplings. To make expressions simpler, in and only in this section we are going to absorb g into the couplings. Formally, this means that every A_{jk} appeared in this section should be understood as gA_{jk} in other sections, and, as a result, every λ_{jk} in this section should be understood as

$$\lambda_{jk} = \sqrt{\frac{\pi}{|b_{jk}|}} g A_{jk}, \quad \text{for } j \neq k. \quad (51)$$

A. Exactly solvable models

The simplest and the most famous model belonging to the one-crossing MLZ class is of course the (two-state)

LZ model. Its Hamiltonian is:

$$H = \begin{pmatrix} b_1 t & A_{12} \\ A_{12} & b_2 t \end{pmatrix}. \quad (52)$$

The exact solutions of its transition probabilities are given by the LZ formula [1-4]:

$$P_{11} = P_{22} = e^{-2\lambda_{12}^2}, \quad (53)$$

$$P_{12} = P_{21} = 1 - e^{-2\lambda_{12}^2}. \quad (54)$$

Here, using (37) and (38) we find the series expansion of P_{12} up to 4th order of A_{12} :

$$P_{12} = 2\lambda_{12}^2 - 2\lambda_{12}^4 + O(g^5), \quad (55)$$

which agrees with the Taylor expansion of the exact result (54).

Besides the LZ model, there are other classes of exactly solvable one-crossing MLZ models. In Table I, we compare the exact solutions of examples of three models — the bow-tie model [10], the γ -magnet model [19, 30], and the driven Tavis-Cummings model [21] — with our perturbative results. In all cases, we find agreement of our results to series expansions of the exact solutions.

B. Models not exactly solved

Below we consider several one-crossing MLZ models which have not been exactly solved. We will write out explicitly probabilities up to 4th order in the couplings. For each model, we perform numerical calculations at different choices of parameters to further confirm the analytical perturbative results.

1. 3-state LZ model with all-to-all couplings

The simplest yet unsolved example would be a one-crossing 3-state LZ model. Its Hamiltonian is:

$$H = \begin{pmatrix} b_1 t & A_{12} & A_{13} \\ A_{12} & b_2 t & A_{23} \\ A_{13} & A_{23} & b_3 t \end{pmatrix}, \quad (56)$$

where $b_1 > b_2 > b_3$. If in addition $b_2 = (b_1 + b_3)/2$, this model describes an $S = 1$ spin under linearly-changing magnetic field in the z -direction with arbitrary couplings between the three states. When any of the three couplings A_{12} , A_{13} , A_{23} is zero, the model belongs to the exactly-solvable bow-tie model [10] discussed previously. For the general case when all couplings are non-vanishing, exact solution is not known. Here, for transition probabilities up to 4th order in the couplings, we obtain for

TABLE I. Comparison of our perturbative results to exact solutions of the 3-state bow-tie model, the 4-state γ -magnet model, and the 4-state driven Tavis-Cummings model. References to works on the exact solutions are given under the model names. For the Tavis-Cummings model, the parameters are defined as $g_i = g\sqrt{i}$, $p_i = e^{-2\pi g_i^2}$, and $q_i = 1 - p_i$ for $i = 1, 2, 3$.

Model	Hamiltonian	Exact solution	Perturbative solution
3-state bow-tie [10]	$\begin{pmatrix} b_1 t & A_{12} & 0 \\ A_{12} & b_2 t & A_{23} \\ 0 & A_{23} & b_3 t \end{pmatrix}$	$P_{12} = (e^{-\lambda_{12}^2} + e^{-\lambda_{23}^2})(1 - e^{-\lambda_{12}^2})$ $P_{13} = (1 - e^{-\lambda_{12}^2})(1 - e^{-\lambda_{23}^2})$ $P_{23} = (e^{-\lambda_{12}^2} + e^{-\lambda_{23}^2})(1 - e^{-\lambda_{23}^2})$	$P_{12} = 2\lambda_{12}^2 - \lambda_{12}^2(2\lambda_{12}^2 + \lambda_{23}^2) + O(g^5)$ $P_{13} = \lambda_{12}^2\lambda_{23}^2 + O(g^5)$ $P_{23} = 2\lambda_{23}^2 - \lambda_{23}^2(\lambda_{12}^2 + 2\lambda_{23}^2) + O(g^5)$
4-state γ -magnet [19, 30]	$\begin{pmatrix} b_1 t & A_{12} & A_{13} & 0 \\ A_{12} & b_2 t & 0 & -A_{13} \\ A_{13} & 0 & -b_2 t & A_{12} \\ 0 & -A_{13} & A_{12} & -b_1 t \end{pmatrix}$	$P_{12} = P_{34} = e^{-2\lambda_{13}^2}(1 - e^{-2\lambda_{12}^2})$ $P_{13} = P_{24} = 1 - e^{-2\lambda_{13}^2}$ $P_{14} = P_{23} = 0$	$P_{12} = 2\lambda_{12}^2 - 2\lambda_{12}^2(\lambda_{12}^2 + 2\lambda_{13}^2) + O(g^5)$ $P_{13} = 2\lambda_{13}^2 - 2\lambda_{13}^4 + O(g^5)$ $P_{14} = O(g^5)$
4-state driven Tavis-Cummings [21]	$\begin{pmatrix} 3t & \sqrt{3}g_3 & 0 & 0 \\ \sqrt{3}g_3 & 2t & 2g_2 & 0 \\ 0 & 2g_2 & t & \sqrt{3}g_1 \\ 0 & 0 & \sqrt{3}g_1 & 0 \end{pmatrix}$	$P_{12} = q_3(p_2^2 + p_2p_3 + p_3^2)$ $P_{13} = q_2q_3(p_1 + p_2 + p_3)$ $P_{14} = q_1q_2q_3$	$P_{12} = 18\pi g^2 - 234\pi^2 g^4 + O(g^5)$ $P_{13} = 72\pi^2 g^4 + O(g^5)$ $P_{14} = O(g^6)$

the off-diagonal elements:

$$P_{12} = 2\lambda_{12}^2 - 2\lambda_{12}\lambda_{13}\lambda_{23} + \lambda_{13}^2\lambda_{23}^2 - \lambda_{12}^2(3\lambda_{13}^2 + \lambda_{23}^2 + 2\lambda_{12}^2) + O(g^5), \quad (57)$$

$$P_{13} = 2\lambda_{13}^2 + 2\lambda_{12}\lambda_{13}\lambda_{23} + \lambda_{12}^2\lambda_{23}^2 - \lambda_{13}^2(\lambda_{12}^2 + \lambda_{23}^2 + 2\lambda_{13}^2) + O(g^5), \quad (58)$$

$$P_{23} = 2\lambda_{23}^2 - 2\lambda_{12}\lambda_{13}\lambda_{23} + \lambda_{12}^2\lambda_{13}^2 - \lambda_{23}^2(\lambda_{12}^2 + 3\lambda_{13}^2 + 2\lambda_{23}^2) + O(g^5), \quad (59)$$

and for the diagonal elements:

$$P_{11} = 1 - 2(\lambda_{12}^2 + \lambda_{13}^2) + 2(\lambda_{12}^2 + \lambda_{13}^2)^2 + O(g^6), \quad (60)$$

$$P_{22} = 1 - 2(\lambda_{12}^2 + \lambda_{23}^2) + 2(\lambda_{12}^2\lambda_{13}^2 + \lambda_{12}^2\lambda_{23}^2 + \lambda_{13}^2\lambda_{23}^2 + \lambda_{12}^4 + \lambda_{23}^4) + O(g^6), \quad (61)$$

$$P_{33} = 1 - 2(\lambda_{13}^2 + \lambda_{23}^2) + 2(\lambda_{13}^2 + \lambda_{23}^2)^2 + O(g^6). \quad (62)$$

Due to the symmetric properties, P_{21} , P_{31} and P_{32} can be obtained by changing the signs of the 3rd order terms in P_{12} , P_{13} and P_{23} , respectively. Note that P_{12} and P_{23} are connected to each other by switching of indices $1 \leftrightarrow 3$, and so are P_{11} and P_{33} .

To check the validity of these analytical expressions of the series expansion of transition probabilities, we performed numerical simulations of the Schrödinger equation of the model (56). Comparison of the analytical series expansion results and numerical results for two transition probabilities are shown in Fig. 4 at one set of randomly chosen parameters. Fig. 4(a) plots P_{12} from numerics and from the series expansion, i.e. Eq. (57). Their agreement at small g confirms the series expansion expressions of P_{12} . As a more accurate check, in Fig. 4(b) we plot the ratio $\Delta P_{12}/g^5$, where ΔP_{12} is the numerically obtained P_{12} subtracted by terms from the analytical series expansion expression (57) up to g^4 . The

fact that this ratio approaches a constant at small g indicates that the difference is of the order of g^5 , which confirms the correctness of Eq. (57). (If any expansion coefficients of the numerical result up to g^4 were different from Eq. (57), that ratio would diverge at $g \rightarrow 0$.) Fig. 4(c) and (d) are similar to Fig. 4(a) and (b) but for P_{22} . Note that in Fig. 4(d) the ratio $\Delta P_{22}/g^6$ is plotted, since P_{22} , being a diagonal element, has a zero expansion coefficient in g^6 .

More numerics are performed at other choices of parameters: a different random choice as shown in Fig. 5(a) and (b), and a “uniform” choice (with uniform couplings and equal slope differences between adjacent levels) as shown in Fig. 5(c) and (d). They all show that the perturbative results agree with the numerical results at small g . Moreover, we see that the values of g above which perturbative results have visible deviation from numerical results are roughly at or slightly above $g = 0.1$ (also see the footnote [57]).

Besides the numerical tests, we also compare the series expansion results with the Brundobler-Elser (BE) formula [35–37], which says that for any MLZ model, the probabilities to stay on the levels with extremal slopes take exact analytical forms. For a general one-crossing MLZ model (namely, a model (1) with $E(t)$ given by (35) and g set to 1) and in terms of λ_{ij} defined in (51), the BE formula predicts:

$$P_{11} = e^{-2\sum_{l=1}^N \lambda_{1l}^2}, \quad (63)$$

$$P_{NN} = e^{-2\sum_{l=1}^N \lambda_{lN}^2}. \quad (64)$$

(The LZ formula can be viewed as a special case of the BE formula at $N = 2$.) Here for the 3-state model (56), we have

$$P_{11} = e^{-2(\lambda_{12}^2 + \lambda_{13}^2)}, \quad (65)$$

$$P_{33} = e^{-2(\lambda_{13}^2 + \lambda_{23}^2)}. \quad (66)$$

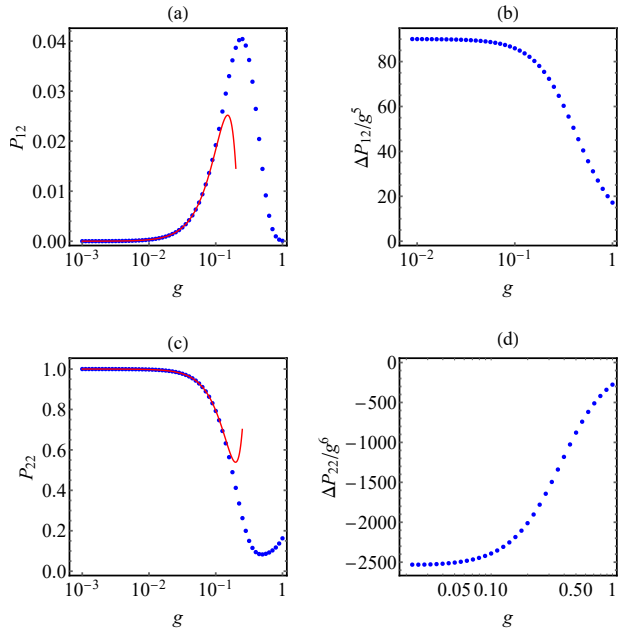


FIG. 4. Comparison of analytical series expansions and numerical results of transition probabilities of the 3-state LZ model (56) at parameter choices $A_{12} = g$, $A_{13} = 1.5g$, $A_{23} = 1.8g$, $b_1 = 2$, $b_2 = 0$, and $b_3 = -1$. (a) P_{12} vs. g from numerical calculations (the dots) and from the series expansion expression (57) (the curve). (b) $\Delta P_{12}/g^5$ vs. g , where ΔP_{12} is the difference of the numerically obtained P_{12} and the series expansion expression (57). (c) P_{22} vs. g from numerical calculations (the dots) and from the series expansion expression (61) (the curve). (d) $\Delta P_{22}/g^6$ vs. g , where ΔP_{22} is the difference of the numerically obtained P_{22} and the series expansion expression (61).

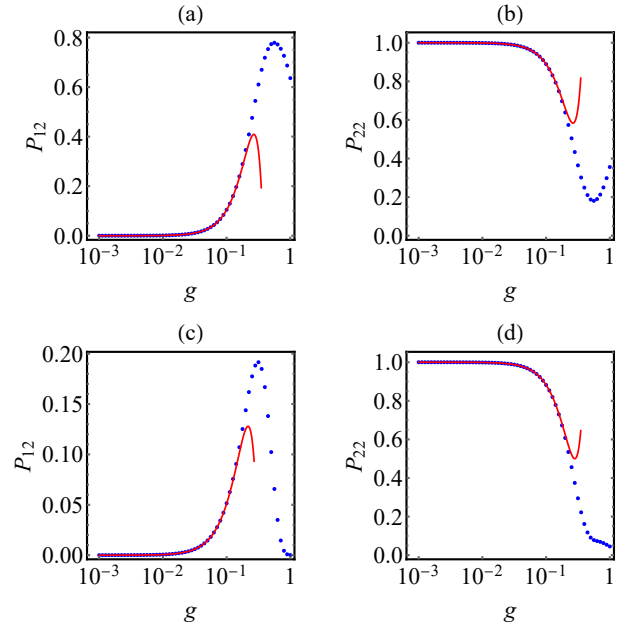


FIG. 5. Comparison of analytical series expansions (the curves) and numerical results (the dots) of transition probabilities of the 3-state LZ model (56) at two other parameter choices. (a) and (b) are at parameters $A_{12} = -1.5g$, $A_{13} = 1.1g$, $A_{23} = 0.4g$, $b_1 = 1.3$, $b_2 = 0$, and $b_3 = -1$. (a) P_{12} vs. g with series expansion given by (57). (b) P_{22} vs. g with series expansion given by (61). (c) and (d) are the same as (a) and (b), respectively, except that the parameters are $A_{12} = A_{13} = A_{23} = g$, $b_1 = 1$, $b_2 = 0$, and $b_3 = -1$.

Performing Taylor expansions of these two exact results, one sees that (60) and (62) for P_{11} and P_{33} do agree with them.

We expect these perturbative results of the 3-state model to be practically useful when considering the dynamics of a spin-1 nanomagnet under a linear sweep of magnetic field. When such a sweep is fast enough (namely in the diabatic limit) our analytical results apply, and they provide theoretical estimates of the excitation probabilities of the spin under the sweep (such analytical estimates have not been achieved by any other theoretical methods), which can further guide experiments on nanomagnets.

2. A 4-state LZ model

We next consider a one-crossing 4-state LZ model, with a Hamiltonian:

$$H = \begin{pmatrix} b_1 t & 0 & A_{13} & A_{14} \\ 0 & b_2 t & A_{23} & A_{24} \\ A_{13} & A_{23} & b_3 t & 0 \\ A_{14} & A_{24} & 0 & b_4 t \end{pmatrix}, \quad (67)$$

where $b_1 > b_2 > b_3 > b_4$. In this model two out of the six couplings are zero. We obtain:

$$P_{12} = (\lambda_{13}\lambda_{23} + \lambda_{14}\lambda_{24})^2 + O(g^5), \quad (68)$$

$$P_{13} = 2\lambda_{13}^2 - \lambda_{13}^2(3\lambda_{14}^2 + \lambda_{23}^2 + 2\lambda_{13}^2) - 4\lambda_{13}\lambda_{14}\lambda_{23}\lambda_{24} + O(g^5), \quad (69)$$

$$P_{14} = 2\lambda_{14}^2 - \lambda_{14}^2(\lambda_{12}^2 + \lambda_{13}^2 + \lambda_{24}^2 + 2\lambda_{14}^2) + 2\lambda_{13}\lambda_{14}\lambda_{23}\lambda_{24} + O(g^5). \quad (70)$$

$$P_{23} = 2\lambda_{23}^2 - \lambda_{23}^2(3\lambda_{24}^2 + 3\lambda_{13}^2 + 2\lambda_{23}^2) - 2\lambda_{13}\lambda_{14}\lambda_{23}\lambda_{24} + O(g^5), \quad (71)$$

$$P_{11} = 1 - 2(\lambda_{13}^2 + \lambda_{14}^2) + 2(\lambda_{13}^2 + \lambda_{14}^2)^2 + O(g^6), \quad (72)$$

$$P_{22} = 1 - 2(\lambda_{23}^2 + \lambda_{24}^2) + \lambda_{23}^2(2\lambda_{13}^2 + 3\lambda_{24}^2 + 2\lambda_{23}^2) + \lambda_{24}^2(2\lambda_{14}^2 + \lambda_{23}^2) + 2\lambda_{24}^4 + 4\lambda_{13}\lambda_{14}\lambda_{23}\lambda_{24} + O(g^6). \quad (73)$$

Again, other P_{jk} with $j \leq k$ are connected to these explicitly written out ones by switches of indices $1 \leftrightarrow 4$ and $2 \leftrightarrow 3$ everywhere, and P_{jk} with $j > k$ can be obtained by changing the signs of the 3rd order terms in P_{kj} . Comparisons to numerics at two sets of parameters are shown in Fig. 6, which again show agreement at small g ($g \lesssim 0.1$). Besides, P_{11} in (72) agrees with the exact result from the BE formula.

For the most general one-crossing 4-state LZ model with all-to-all couplings, the expressions of probabilities also straightforwardly follow from Eqs. (37)-(41), but are more complicated. We present results of that more general model in the supplemental material.

3. A 5-state LZ model

We next consider a one-crossing 5-state LZ model with the following Hamiltonian

$$H = \begin{pmatrix} -b_1 t & A_{12} & A_{13} & A_{14} & 0 \\ A_{12} & -b_2 t & 0 & 0 & -A_{14} \\ A_{13} & 0 & 0 & 0 & -A_{13} \\ A_{14} & 0 & 0 & b_2 t & -A_{12} \\ 0 & -A_{14} & -A_{13} & -A_{12} & b_1 t \end{pmatrix}, \quad (74)$$

where $b_2 > b_1 > 0$. This model is related to a 5-site Su-Schrieffer-Heeger chain under a linear quench of its couplings, and was studied in detail in [2]. Its exact solution has not been found, but by analytical constraint method it was shown in [2] that all of its transition probabilities depends only on two of them, for example, P_{32} and P_{33} . Here we obtain for these two probabilities (note that since the levels in the Hamiltonian (74) are not in descending order of the slopes, they should be reordered before applying Eqs. (37)-(41)):

$$P_{32} = \lambda_{13}^2(\lambda_{12}^2 + \lambda_{14}^2) + O(g^5), \quad (75)$$

$$P_{33} = 1 - 4\lambda_{13}^2 + 2\lambda_{13}^2(3\lambda_{13}^2 + 2\lambda_{14}^2) + O(g^6). \quad (76)$$

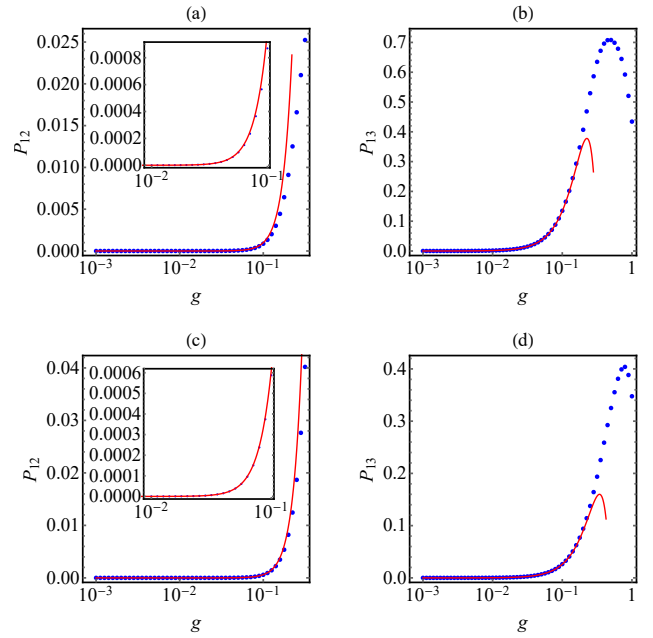


FIG. 6. Comparison of analytical series expansions (the curves) and numerical results (the dots) of transition probabilities of the 4-state LZ model (67) at two parameter choices. (a) and (b) are at parameters $A_{13} = 3g$, $A_{23} = g$, $A_{14} = -1.5g$, $A_{24} = 0.4g$, $b_1 = 3$, $b_2 = 1$, $b_3 = -0.8$, and $b_4 = -2.4$. (a) P_{12} vs. g with series expansion given by (68); the inset shows the same curve zoomed into the region $0.01 < g < 0.1$. (b) P_{22} vs. g with series expansion given by (69). (c) and (d) are the same as (a) and (b), respectively, except that the parameters are $A_{13} = -g$, $A_{23} = 1.2g$, $A_{14} = 0.4g$, $A_{24} = -0.7g$, $b_1 = 1.5$, $b_2 = 0.5$, $b_3 = -0.8$, and $b_4 = -2$.

By numerical calculations at different choices of parameters, the series expansion of $|S_{32}|$ and S_{33} was found in [2] (see Eqs. (52) and (53) there). Taking squares of them, we find that they do agree with (75) and (76) here. Hence, the series expansions previously found from numerics can now be derived analytically.

4. A 6-state chain model

As a final example, we consider a 6-state chain model with a Hamiltonian:

$$H = \begin{pmatrix} b_1 t & A_{12} & 0 & 0 & 0 & 0 \\ A_{12} & b_2 t & A_{23} & 0 & 0 & 0 \\ 0 & A_{23} & b_3 t & A_{34} & 0 & 0 \\ 0 & 0 & A_{34} & b_4 t & A_{45} & 0 \\ 0 & 0 & 0 & A_{45} & b_5 t & A_{56} \\ 0 & 0 & 0 & 0 & A_{56} & b_6 t \end{pmatrix}. \quad (77)$$

In Section IIID, we determined transition probabilities up to 4th-order in couplings for a general N -state chain model. Here we compare these perturbative results to

numerics for a 6-state chain model with uniform couplings and equal slope differences between adjacent levels in Fig. 7. Again, one see agreement between the two at small g ($g \lesssim 0.1$).

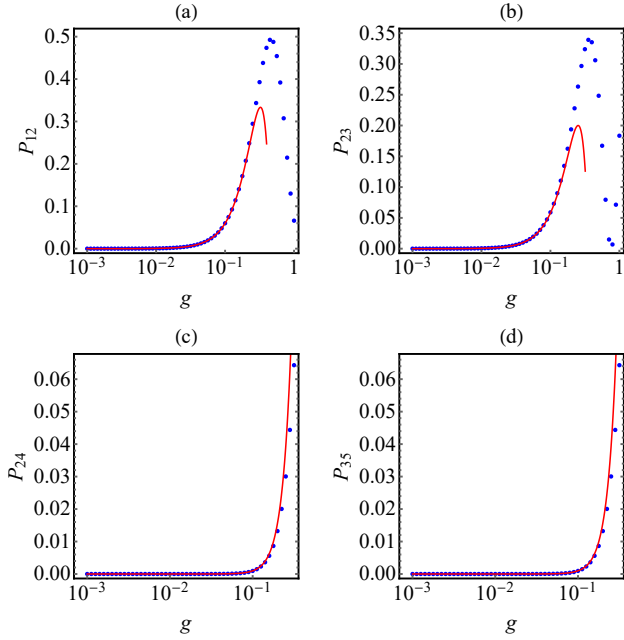


FIG. 7. Comparison of analytical series expansions (the curves) and numerical results (the dots) of transition probabilities of the 6-state chain model (77) at the parameter choices $A_{j,j+1} = g$ ($j = 1, 2, 3, 4, 5$), $b_1 = 2.5$, $b_2 = 1.5$, $b_3 = 0.5$, and $b_4 = -0.5$, $b_5 = -1.5$, $b_6 = -2.5$ for (a) P_{12} vs. g ; (b) P_{23} vs. g ; (c) P_{24} vs. g ; (d) P_{35} vs. g .

V. CONCLUSIONS AND DISCUSSIONS

We formulated a perturbative approach that applies to a general time-dependent quantum system with constant off-diagonal couplings and diabatic energies being

odd functions of time. Using this approach for a general MLZ model with all levels crossing at a single point (one-crossing MLZ model), we derived analytical expressions of all its transition probabilities up to 4th order in the couplings (Eqs. (37)-(41) in Section IIIA), which become asymptotically exact at the diabatic limit. These expressions depend on the couplings A_{jk} and the slopes b_j solely via the combinations $A_{jk}/\sqrt{|b_j - b_k|}$. To our best knowledge, such analytical results haven't been achieved by any other approximation methods for one-crossing MLZ models not exactly solvable. These analytical asymptotic solutions at the diabatic limit can serve as reliable references for future studies of any unsolved one-crossing MLZ models; for example, transition probabilities for any one-crossing MLZ model found in future studies by any method must have series expansions which agree with the results here.

Let us discuss possible future extensions of this work. One direction is of course trying to derive analytical expressions of higher order expansions of probabilities for one-crossing MLZ models, although we expect that calculations may be very involved (given the complexity of the performed calculations of 4th order terms). Second, in this work we focused on MLZ models, namely, models with linear time dependence. But recall that the perturbative approach can be applied to a model with a more general time-dependence of its diabatic energies as long as they are odd in time. One may thus also consider models with diabatic energies of forms t^3 or $\sinh t$, etc., and the series expansion of transition probabilities are expected to be expressed in terms of multiple integrals of different forms corresponding to the specific time dependencies. Third, probabilities at finite instead of infinite times may also be considered.

ACKNOWLEDGEMENTS

This work was supported by the National Natural Science Foundation of China under Grant No. 12105094, and by the Fundamental Research Funds for the Central Universities from China.

[1] L. Landau, Zur Theorie der Energieübertragung. II, *Phys. Z. Sowj.* **2**, 46 (1932).

[2] C. Zener. Non-Adiabatic Crossing of Energy Levels, *Proc. R. Soc.* **137**, 696 (1932).

[3] E. Majorana, Atomi orientati in campo magnetico variabile, *Nuovo Cimento* **9**, 43 (1932).

[4] E. C. G. Stückelberg. Theorie der unelastischen Stöße zwischen Atomen, *Helv. Phys. Acta* **5**, 370 (1932).

[5] S. N. Shevchenko, S. Ashhab, and F. Nori, Landau-Zener-Stückelberg interferometry, *Phys. Rep.* **492**, 1 (2010).

[6] O. V. Ivakhnenko, S. N. Shevchenko, and F. Nori, Non-adiabatic Landau-Zener-Stückelberg-Majorana transitions, dynamics, and interference, *Phys. Rep.* **995**, 1 (2023).

[7] J. Wei and E. Norman, Lie Algebraic Solution of Linear Differential Equations, *J. Math. Phys.* **4**, 575 (1963).

[8] Yu. N. Demkov and V. I. Osherov, *Zh. Eksp. Teor. Fiz.* **53**, 1589 (1967) [Stationary and nonstationary problems in quantum mechanics that can be solved by means of contour integration, *Sov. Phys. JETP* **26**, 916 (1968)].

[9] F. T. Hioe, *N*-level quantum systems with $SU(2)$ dynamic symmetry, *J. Opt. Soc. Am. B* **4**, 1327 (1987).

[10] V. N. Ostrovsky and H. Nakamura, Exact analytical solution of the N -level Landau-Zener-type bow-tie model, *J. Phys. A: Math. Gen.* **30**, 6939 (1997).

[11] A. R. P. Rau, Unitary Integration of Quantum Liouville-Bloch Equations, *Phys. Rev. Lett.* **81**, 4785 (1998).

[12] Y. N. Demkov and V. N. Ostrovsky, Multipath interference in a multistate Landau-Zener-type model, *Phys. Rev. A* **61**, 032705 (2000).

[13] Y. N. Demkov and V. N. Ostrovsky, The exact solution of the multistate Landau-Zener type model: the generalized bow-tie model, *J. Phys. B: At. Mol. Opt. Phys.* **34**, 2419 (2001).

[14] A. R. P. Rau and W. Zhao, Decoherence in a driven three-level system, *Phys. Rev. A* **68**, 052102 (2003).

[15] A. R. P. Rau, G. Selvaraj, and D. Uskov, Four-level and two-qubit systems, subalgebras, and unitary integration, *Phys. Rev. A* **71**, 062316 (2005).

[16] A. R. P. Rau and W. Zhao, Time-dependent treatment of a general three-level system, *Phys. Rev. A* **71**, 063822 (2005).

[17] G. S. Vasilev, S. S. Ivanov, and N. V. Vitanov, Degenerate Landau-Zener model: Analytical solution, *Phys. Rev. A* **75**, 013417 (2007).

[18] N. A. Sinitzyn, Landau-Zener transitions in chains, *Phys. Rev. A* **87**, 032701 (2013).

[19] N. A. Sinitzyn, Solvable four-state Landau-Zener model of two interacting qubits with path interference, *Phys. Rev. B* **92**, 205431 (2015).

[20] N. A. Sinitzyn, Exact transition probabilities in a 6-state Landau-Zener system with path interference, *J. Phys. A: Math. Theor.* **48**, 195305 (2015).

[21] N. A. Sinitzyn and F. Li, Solvable multistate model of Landau-Zener transitions in cavity QED, *Phys. Rev. A* **93**, 063859 (2016).

[22] C. Sun and N. A. Sinitzyn, Landau-Zener extension of the Tavis-Cummings model: Structure of the solution, *Phys. Rev. A* **94**, 033808 (2016).

[23] N. A. Sinitzyn, J. Lin, and V. Y. Chernyak, Constraints on scattering amplitudes in multistate Landau-Zener theory, *Phys. Rev. A* **95**, 012140 (2017).

[24] F. Li, C. Sun, V. Y. Chernyak, and N. A. Sinitzyn, Multistate Landau-Zener models with all levels crossing at one point, *Phys. Rev. A* **96**, 022107 (2017).

[25] A. Patra and E. A. Yuzbashyan, Quantum integrability in the multistate Landau-Zener problem, *J. Phys. A: Math. Theor.* **48**, 245303 (2015).

[26] N. A. Sinitzyn and V. Y. Chernyak, The quest for solvable multistate Landau-Zener models, *J. Phys. A: Math. Theor.* **50**, 255203 (2017).

[27] V. Y. Chernyak, N. A. Sinitzyn, and C. Sun, A large class of solvable multistate Landau-Zener models and quantum integrability, *J. Phys. A: Math. Theor.* **51**, 245201 (2018).

[28] N. A. Sinitzyn, E. A. Yuzbashyan, V. Y. Chernyak, A. Patra, and C. Sun, Integrable time-dependent quantum Hamiltonians, *Phys. Rev. Lett.* **120**, 190402 (2018).

[29] E. A. Yuzbashyan, Integrable time-dependent Hamiltonians, solvable Landau-Zener models and Gaudin magnets, *Ann. Phys.* **392**, 323 (2018).

[30] Dynamic spin localization and γ -magnets, V. Y. Chernyak, N. A. Sinitzyn, and C. Sun, *Phys. Rev. B* **100**, 224304 (2019).

[31] V. Y. Chernyak, N. A. Sinitzyn, and C. Sun, Multitime Landau-Zener model: classification of solvable Hamiltonians, *J. Phys. A: Math. Theor.* **53**, 185203 (2020).

[32] V. Y. Chernyak, F. Li, C. Sun, and N. A. Sinitzyn, Integrable multistate Landau-Zener models with parallel energy levels, *J. Phys. A: Math. Theor.* **53**, 295201 (2020).

[33] V. Y. Chernyak and N. A. Sinitzyn, Integrability in the multistate Landau-Zener model with time-quadratic com- muting operators, *J. Phys. A: Math. Theor.* **54**, 115204 (2021).

[34] R. K. Malla, J. Cen, W. J. M. Kort-Kamp, and A. Saxena, Quantum dynamics of non-Hermitian many-body Landau-Zener systems, *Phys. Rev. A* **108**, 062217 (2023).

[35] S. Brundobler and V. Elser, S-matrix for generalized Landau-Zener problem, *J. Phys. A: Math. Gen.* **26**, 1211 (1993).

[36] N. A. Sinitzyn, Counterintuitive transitions in the multistate Landau-Zener problem with linear level crossings, *J. Phys. A: Math. Gen.* **37**, 10691 (2004).

[37] A. V. Shytov, Landau-Zener transitions in a multilevel system: An exact result, *Phys. Rev. A* **70**, 052708 (2004).

[38] T. Usuki, Theoretical study of Landau-Zener tunneling at the M - N level crossing, *Phys. Rev. B* **56**, 13360 (1997).

[39] M. Wubs, K. Saito, S. Kohler, P. Hänggi, and Y. Kyanuma, Gauging a Quantum Heat Bath with Dissipative Landau-Zener Transitions *Phys. Rev. Lett.* **97**, 200404 (2006).

[40] K. Saito, M. Wubs, S. Kohler, Y. Kyanuma, and P. Hänggi, Dissipative Landau-Zener transitions of a qubit: Bath-specific and universal behavior, *Phys. Rev. B* **75**, 214308 (2007).

[41] When there are more than one such paths, one also needs to appropriately take into account interference of them due to their phases.

[42] T. Suzuki, E. Taniguchi, and K. Iwamura, Exact WKB analysis for adiabatic discrete-level Hamiltonians, *Phys. Rev. A* **109**, 022225 (2024).

[43] T. Aoki, T. Kawai and Y. Takei, Exact WKB analysis of non-adiabatic transition probabilities for three levels, *J. Phys. A: Math. Gen.* **35**, 2401 (2002).

[44] N. Shimada and A. Shudo, Numerical verification of the exact WKB formula for the generalized Landau-Zener-Stueckelberg problem, *Phys. Rev. A* **102**, 022213 (2020).

[45] A. M. Dykhne, Adiabatic perturbation of discrete spectrum states, *Sov. Phys. JETP* **14**, 941 (1962).

[46] J. P. Davis and P. Pechukas, Nonadiabatic transitions induced by a time-dependent Hamiltonian in the semiclassical/adiabatic limit: the two-state case. *J. Chem. Phys.* **64**, 3129 (1976).

[47] K. Fukushima and T. Shimazaki, Lefschetz-thimble inspired analysis of the Dykhne-Davis-Pechukas method and an application for the Schwinger Mechanism, *Ann. Phys., NY* **415**, 168111 (2020).

[48] J.-T. Hwang and P. Pechukas, The adiabatic theorem in the complex plane and the semiclassical calculation of nonadiabatic transition amplitudes, *J. Chem. Phys.* **67**, 4640 (1977).

[49] S. Ashhab, Landau-Zener transitions in an open multilevel quantum system, *Phys. Rev. A* **94**, 042109 (2016).

[50] A. Niranjan, W. Li, and R. Nath, Landau-Zener transitions and adiabatic impulse approximation in an array of two Rydberg atoms with time-dependent detuning, *Phys. Rev. A* **101**, 063415 (2020).

[51] R. Hu, F. Li, and C. Sun, Solution to a class of multistate Landau-Zener model beyond integrability conditions, *Phys. Scr.* **99**, 065226 (2024).

[52] W. La Cava, P. Orzechowski, B. Burlacu, F. O. de Franca, M. Virgolin, Y. Jin, M. Kommenda, and J. H. Moore, Contemporary Symbolic Regression Methods and their Relative Performance, arXiv:2107.14351 [cs.NE] 29 Jul 2021.

- [53] S.-M. Udrescu and M. Tegmark, AI Feynman: A physics-inspired method for symbolic regression, *Sci. Adv.* **6**, 2631 (2020).
- [54] S.-M. Udrescu, A. Tan, J. Feng, O. Neto, T. Wu, and M. Tegmark, AI Feynman 2.0: Pareto-optimal symbolic regression exploiting graph modularity, In Proceedings of the 34th Conference on Neural Information Processing Systems (NeurIPS 2020), Vancouver, BC, Canada, 6-12 December 2020; pp. 1-12.
- [55] S. Ashhab, Using machine learning to find exact analytic solutions to analytically posed physics problems, *Heliyon*, **10**, 6 (2024).
- [56] W. Wernsdorfer and R. Sessoli, Quantum Phase Interference and Parity Effects in Magnetic Molecular Clusters, *Science* **284**, 133 (1999).
- [57] We make precise what is the meaning of the diabatic limit, or “small g ”. For one-crossing MLZ models discussed later, it means that all the LZ parameters $(gA_{jk})^2/|b_j - b_k|$ are much smaller than 1, so that g is much smaller than a value $g_c \sim \min(\sqrt{|b_j - b_k|/|A_{jk}|})$. For the more general model Eq. (1), $|b_j - b_k|$ should be replaced by the values of $|\partial(\varepsilon_j - \varepsilon_k)/\partial t|$ at the crossing of diabatic levels. If we take both the couplings A_{jk} and the slope differences $|b_j - b_k|$ to be of the order of 1 (recall that in our units system they are all dimensionless), then small g simply means $g \ll 1$.
- [58] D. Waxman, Perturbative Approach to Landau-Zener Transitions, *Ann. Phys. (NY)*, **236**, 205 (1994).

Supplemental Material for ‘‘Perturbative approach to time-dependent quantum systems and applications to one-crossing multistate Landau-Zener models’’

APPENDIX A: DERIVATION OF THE PROBABILITIES FOR ONE-CROSSING MLZ MODELS

In this Appendix, we are going to calculate explicitly the matrix elements of P_n of the general one-crossing MLZ model (the model (1) with $E(t)$ given by (35) in the main text) up to $n = 4$, namely, transition probabilities up to 4th order in the couplings. Our calculation procedures are presented in a sufficiently detailed manner so readers interested in reproducing them can readily do so.

Note that due to the symmetry properties (30) and (31) in the main text, it suffices to determine those elements $P_{n,jk}$ with $j \leq k$.

1. Probabilities up to g^3

We start by writing out the matrix elements of $W_1(t)$, $W_2(t)$, and $W_3(t)$ explicitly:

$$W_{1,jk}(t) = -2i \int_0^t ds \tilde{A}_{jk}(s), \quad (\text{A1})$$

$$W_{2,jk}(t) = -2 \left\{ \left[\int_0^t ds \tilde{A}(s) \right]^2 \right\}_{jk}, \quad (\text{A2})$$

$$W_{3,jk}(t) = 2i \left\{ \left[\int_0^t ds \tilde{A}(s) \right]^3 \right\}_{jk} - 2i \sum_{l,p} \int_0^t ds \left[\int_0^s ds_1 \tilde{A}_{jl}(s_1) \right] \tilde{A}_{lp}(s) \left[\int_0^s ds_1 \tilde{A}_{pk}(s_1) \right]. \quad (\text{A3})$$

Recall that $\tilde{A}_{jj}(t) = 0$ and $\tilde{A}_{jk}(t) = e^{i(\phi_j(t) - \phi_k(t))} A_{jk}$ for $j \neq k$. The phase $\phi_j(t)$ reads:

$$\phi_j(t) = \int_0^t ds b_j s = \frac{1}{2} b_j t^2. \quad (\text{A4})$$

So

$$\int_0^t ds \tilde{A}_{jk}(s) = A_{jk} \int_0^t ds e^{i \frac{1}{2} b_{jk} s^2} = A_{jk} \sqrt{\frac{\pi}{|b_{jk}|}} \left[C \left(\sqrt{\frac{|b_{jk}|}{\pi}} t \right) + i \operatorname{sgn}(b_{jk}) S \left(\sqrt{\frac{|b_{jk}|}{\pi}} t \right) \right], \quad (\text{A5})$$

where sgn is the sign function, the slope differences are denoted as

$$b_{jk} \equiv b_j - b_k \quad (\text{A6})$$

for notation simplicity, and $C(x)$ and $S(x)$ ($x \geq 0$) are the Fresnel integrals [1] defined as

$$C(x) = \int_0^x \cos \left(\frac{\pi}{2} t^2 \right) dt, \quad (\text{A7})$$

$$S(x) = \int_0^x \sin \left(\frac{\pi}{2} t^2 \right) dt. \quad (\text{A8})$$

Let’s now determine the matrix elements of P_n up to $n = 3$. For this purpose, it suffices to consider $W_1(\infty)$ and $W_2(\infty)$. Using limits of the Fresnel integrals at infinity

$$C(\infty) = S(\infty) = \frac{1}{2}, \quad (\text{A9})$$

one arrives at

$$\int_0^\infty ds \tilde{A}_{jk}(s) = \sqrt{\frac{\pi}{2|b_{jk}|}} e^{i \frac{\pi}{4} \operatorname{sgn}(b_{jk})} A_{jk} = \frac{1}{\sqrt{2}} \lambda_{jk} e^{i \frac{\pi}{4} \operatorname{sgn}(b_{jk})}, \quad (\text{A10})$$

where we defined the combinations

$$\lambda_{jk} = \sqrt{\frac{\pi}{|b_{jk}|}} A_{jk}, \quad \text{for } j \neq k. \quad (\text{A11})$$

These combinations will appear frequently during our analysis. Later, whenever possible, expressions will be written in terms of these λ_{jk} . From (A10), $W_1(\infty)$ follows immediately:

$$W_{1,jj}(\infty) = 0, \quad (\text{A12})$$

$$W_{1,jk}(\infty) = -i\sqrt{2}\lambda_{jk}e^{i\frac{\pi}{4}}, \quad \text{for } j < k. \quad (\text{A13})$$

$W_2(\infty)$ involves a sum

$$W_{2,jk}(\infty) = -\sum_l \lambda_{jl} \lambda_{lk} e^{i\frac{\pi}{4}[\operatorname{sgn}(b_{jl}) + \operatorname{sgn}(b_{lk})]}. \quad (\text{A14})$$

Let's look at the diagonal and off-diagonal elements of $W_2(\infty)$ separately. For $j = k$ one always has $\operatorname{sgn}(b_{jl}) = -\operatorname{sgn}(b_{lk})$, so

$$W_{2,jj}(\infty) = -\sum_l^{l \neq j} \lambda_{jl}^2. \quad (\text{A15})$$

For $j < k$, if $l < j$ or $l > k$ we have $\operatorname{sgn}(b_{jl}) = -\operatorname{sgn}(b_{lk})$, and if $j < l < k$ we have $\operatorname{sgn}(b_{jl}) = \operatorname{sgn}(b_{lk}) = 1$, so

$$W_{2,jk}(\infty) = -\sum_l^{l < j \text{ or } l > k} \lambda_{jl} \lambda_{lk} - i \sum_l^{j < l < k} \lambda_{jl} \lambda_{lk}. \quad (\text{A16})$$

From $W_1(\infty)$ and $W_2(\infty)$, the transition probabilities can then be determined up to terms with g^3 . The diagonal elements are:

$$P_{jj} = |W_{jj}(\infty)|^2 = 1 - 2g^2 \sum_l^{l \neq j} \lambda_{jl}^2 + O(g^4). \quad (\text{A17})$$

The off-diagonal elements with $j < k$ are:

$$P_{jk} = |W_{jk}(\infty)|^2 = 2g^2 \lambda_{jk}^2 - 2g^3 \lambda_{jk} \left(\sum_l^{l < j \text{ or } l > k} \lambda_{jl} \lambda_{lk} - \sum_l^{j < l < k} \lambda_{jl} \lambda_{lk} \right) + O(g^4). \quad (\text{A18})$$

2. Probabilities in g^4

Below we determine terms in g^4 for the transition probabilities, which analysis is more complicated. Let's first consider the off-diagonal elements $P_{4,jk}$ with $j < k$. We need to calculate $W_{3,jk}(\infty)$, which reads

$$W_{3,jk}(\infty) = 2i \left\{ \left[\int_0^\infty ds \tilde{A}(s) \right]^3 \right\}_{jk} - 2i \sum_{l,p} \int_0^\infty ds \left[\int_0^s ds_1 \tilde{A}_{jl}(s_1) \right] \tilde{A}_{lp}(s) \left[\int_0^s ds_1 \tilde{A}_{pk}(s_1) \right]. \quad (\text{A19})$$

The integrals in the first term in (A19) can be evaluated similarly as $W_{1,jk}(\infty)$ and $W_{2,jk}(\infty)$ using the limits of Fresnel integrals:

$$\left\{ \left[\int_0^\infty ds \tilde{A}(s) \right]^3 \right\}_{jk} = \frac{1}{2\sqrt{2}} \sum_{l,p} \lambda_{jl} \lambda_{lp} \lambda_{pk} e^{i\frac{\pi}{4}[\operatorname{sgn}(b_{jl}) + \operatorname{sgn}(b_{lp}) + \operatorname{sgn}(b_{pk})]} = \left(\frac{\pi}{2} \right)^{\frac{3}{2}} \sum_{l,p} \frac{A_{jl} A_{lp} A_{pk}}{\sqrt{-ib_{jl}} \sqrt{-ib_{lp}} \sqrt{-ib_{pk}}}, \quad (\text{A20})$$

where in the last equality we used the fact that b_{jl} is a non-zero real number, so

$$\sqrt{-ib_{jl}} = \sqrt{|b_{jl}|} e^{-i\frac{\pi}{4} \operatorname{sgn}(b_{jl})}, \quad (\text{A21})$$

and similarly for b_{lp} and b_{pk} (the branch cut of a square root function is taking to be slightly below the negative real axis).

Evaluation of the second term in (A19) takes much more efforts. It is a sum of terms of the form

$$\int_0^\infty ds \tilde{A}_{lp}(s) \int_0^s ds_1 \tilde{A}_{jl}(s_1) \int_0^s ds_2 \tilde{A}_{pk}(s_2) \equiv A_{jl} A_{lp} A_{pk} Q, \quad (\text{A22})$$

where Q is the following integral:

$$\begin{aligned} Q &= \int_0^\infty ds e^{i\frac{1}{2}b_{lp}s^2} \int_0^s ds_1 e^{i\frac{1}{2}b_{jl}s_1^2} \int_0^s ds_2 e^{i\frac{1}{2}b_{pk}s_2^2} \\ &= \frac{\pi}{\sqrt{|b_{jl}b_{pk}|}} \int_0^\infty ds e^{i\frac{1}{2}b_{lp}s^2} \left[C\left(\sqrt{\frac{|b_{jl}|}{\pi}}s\right) + i \operatorname{sgn}(b_{jl}) S\left(\sqrt{\frac{|b_{jl}|}{\pi}}s\right) \right] \left[C\left(\sqrt{\frac{|b_{pk}|}{\pi}}s\right) + i \operatorname{sgn}(b_{pk}) S\left(\sqrt{\frac{|b_{pk}|}{\pi}}s\right) \right]. \end{aligned} \quad (\text{A23})$$

We find that result of this integral separate into two cases depending on whether the values of the slopes satisfy at least one of $b_{jl} + b_{lp} = 0$ and $b_{lp} + b_{pk} = 0$. We call this condition the “resonance condition”. The case that this condition is not satisfied will be named the “off-resonant” case, and the other case that this condition is satisfied will be named the “resonant” case. Note that $b_{jl} + b_{lp} = 0$ means $p = j$ and $b_{lp} + b_{pk} = 0$ means $l = k$, so the resonance condition is equivalent to saying that at least one of $p = j$ and $l = k$ is satisfied.

In the off-resonant case, this integral (A23) can be evaluated using the parametric integration technique. The procedure is rather complicated so details will be given in a separate Appendix B, and here we present directly the result:

$$Q = \sqrt{\frac{\pi}{2}} \frac{1}{\sqrt{-ib_{jl}} \sqrt{-ib_{lp}} \sqrt{-ib_{pk}}} \left[\theta(-b_{lp}) \theta(b_{jp}) \theta(b_{lk}) \pi + \operatorname{Arctan} \frac{\sqrt{-ib_{jl}} \sqrt{-ib_{pk}}}{\sqrt{-ib_{lp}} \sqrt{-ib_{jk}}} \right], \quad (\text{A24})$$

where $\theta(x)$ is the Heaviside step function, and Arctan is the complex-valued inverse tangent function defined in the principal branch (the branch cuts are taken to lie on the imaginary axis at $(-i\infty, -i]$ and $[-i, i\infty)$; values of Arctan have real parts $\pi/2$ or $-\pi/2$ for points on the upper/lower branch cut, respectively).

In the resonant case, this integral (A23) diverges. This means that the corresponding term in $W_{3,jk}(t)$ does not have a limit at $t \rightarrow \infty$. However, we recall that the probability P_{jk} , what we are interested in, is bounded between 0 and 1 at any value of g , and we expect that it should have a well-defined limit at each order of g . Thus, $P_{jk}(\infty)$ must converge even if $W_{jk}(\infty)$ does not. Let’s look at $P_{4,jk}$ with $j < k$. Since $W_{0,jk}(t)$ vanishes, according to (21) in the main text, the leading order in which $W_{3,jk}$ appears is $P_{4,jk}$, which reads

$$P_{4,jk} = \lim_{t \rightarrow \infty} \{ |W_{2,jk}(t)|^2 + [W_{1,jk}^*(t)W_{3,jk}(t) + c.c.] \}. \quad (\text{A25})$$

Thus, a resonant term contributes to $P_{4,jk}$ via the combination

$$R \equiv \lim_{t \rightarrow \infty} \left\{ \left[-2i \int_0^t ds \tilde{A}_{jk}(s) \right]^* \left[-2i \int_0^t ds \tilde{A}_{lp}(s) \int_0^s ds_1 \tilde{A}_{jl}(s_1) \int_0^s ds_2 \tilde{A}_{pk}(s_2) \right] + c.c. \right\}. \quad (\text{A26})$$

Calculating this limit numerically for different choices b_{jl} , b_{lp} and b_{pk} satisfying the resonance condition, we find that it indeed converges, and the limit is

$$R = \begin{cases} \operatorname{sgn}(b_{lk}) \lambda_{jk}^2 \lambda_{jl}^2, & \text{for } p = j \text{ and } l \neq k, \\ \operatorname{sgn}(b_{jp}) \lambda_{jk}^2 \lambda_{pk}^2, & \text{for } p \neq j \text{ and } l = k, \\ 0, & \text{for } p = j \text{ and } l = k. \end{cases} \quad (\text{A27})$$

All other contributions to $P_{4,jk}$ can be calculated directly using the results obtained above for $W_{1,jk}(\infty)$, $W_{2,jk}(\infty)$, and other terms in $W_{3,jk}(\infty)$. The term $|W_{2,jk}(\infty)|^2$ reads:

$$|W_{2,jk}(\infty)|^2 = \left(\sum_l^{l < j \text{ or } l > k} \lambda_{jl} \lambda_{lk} \right)^2 + \left(\sum_l^{j < l < k} \lambda_{jl} \lambda_{lk} \right)^2. \quad (\text{A28})$$

The first term in (A19), namely the completely symmetric term, gives a contribution:

$$P_{4,jk}^{sym} = -\lambda_{jk} \sum_{l,p} \lambda_{jl} \lambda_{lp} \lambda_{pk} e^{i \frac{\pi}{4} [\operatorname{sgn}(b_{jl}) + \operatorname{sgn}(b_{lp}) + \operatorname{sgn}(b_{pk}) - 1]} + c.c. \quad (\text{A29})$$

The quantity $\operatorname{sgn}(b_{jl}) + \operatorname{sgn}(b_{lp}) + \operatorname{sgn}(b_{pk}) - 1$ can take 3 possible values: 0, and ± 2 . When added with the complex conjugated terms, only terms with $\operatorname{sgn}(b_{jl}) + \operatorname{sgn}(b_{lp}) + \operatorname{sgn}(b_{pk}) - 1 = 0$ survive, so

$$P_{4,jk}^{sym} = -2\lambda_{jk} \sum_{l,p}^{\operatorname{sgn}(b_{jl}) + \operatorname{sgn}(b_{lp}) + \operatorname{sgn}(b_{pk}) = 1} \lambda_{jl} \lambda_{lp} \lambda_{pk}. \quad (\text{A30})$$

The off-resonance terms give a contribution:

$$P_{4,jk}^{off-res} = 2\lambda_{jk} \sum_{l,p}^{p \neq j, l \neq k} \lambda_{jl} \lambda_{lp} \lambda_{pk} e^{i \frac{\pi}{4} [\operatorname{sgn}(b_{jl}) + \operatorname{sgn}(b_{lp}) + \operatorname{sgn}(b_{pk}) - 1]} \left[\theta(-b_{lp}) \theta(b_{jp}) \theta(b_{lk}) \pi + \operatorname{Arctan} \frac{\sqrt{-ib_{jl}} \sqrt{-ib_{pk}}}{\sqrt{-ib_{lp}} \sqrt{-ib_{jk}}} \right] + c.c. \quad (\text{A31})$$

The phase of the argument of Arctan function is

$$\arg \frac{\sqrt{-ib_{jl}} \sqrt{-ib_{pk}}}{\sqrt{-ib_{lp}} \sqrt{-ib_{jk}}} = \frac{\pi}{2} \operatorname{sgn}(b_{lp}) - \frac{\pi}{4} [\operatorname{sgn}(b_{jl}) + \operatorname{sgn}(b_{lp}) + \operatorname{sgn}(b_{pk}) - 1]. \quad (\text{A32})$$

When $\operatorname{sgn}(b_{jl}) + \operatorname{sgn}(b_{lp}) + \operatorname{sgn}(b_{pk}) - 1 = \pm 2$, the exponential phase factor in (A31) is $\pm i$, so the imaginary part of the Arctan function is selected. But according to (A32), $\arg[\sqrt{-ib_{jl}} \sqrt{-ib_{pk}} / (\sqrt{-ib_{lp}} \sqrt{-ib_{jk}})]$ can only be 0 or $\pm \pi$, and the Arctan function is always real, so the contribution vanishes. When $\operatorname{sgn}(b_{jl}) + \operatorname{sgn}(b_{lp}) + \operatorname{sgn}(b_{pk}) - 1 = 0$, the real part of the Arctan function is selected. In this case,

$$\arg \frac{\sqrt{-ib_{jl}} \sqrt{-ib_{pk}}}{\sqrt{-ib_{lp}} \sqrt{-ib_{jk}}} = \frac{\pi}{2} \operatorname{sgn}(b_{lp}), \quad (\text{A33})$$

and for a real x ,

$$\operatorname{Re}[\operatorname{Arctan}(ix)] = \begin{cases} \frac{\pi}{2} \operatorname{sgn}(x), & \text{for } |x| > 1, \\ 0, & \text{for } |x| < 1. \end{cases} \quad (\text{A34})$$

We thus obtain

$$\operatorname{Re} \left[\operatorname{Arctan} \frac{\sqrt{-ib_{jl}} \sqrt{-ib_{pk}}}{\sqrt{-ib_{lp}} \sqrt{-ib_{jk}}} \right] = \frac{\pi}{2} \theta(-b_{jp} b_{lk}) \operatorname{sgn}(b_{lp}). \quad (\text{A35})$$

Therefore, the off-resonance contribution reads:

$$P_{4,jk}^{off-res} = 4\lambda_{jk} \sum_{l,p, p \neq j, l \neq k}^{\operatorname{sgn}(b_{jl}) + \operatorname{sgn}(b_{lp}) + \operatorname{sgn}(b_{pk}) = 1} \lambda_{jl} \lambda_{lp} \lambda_{pk} \left[\theta(-b_{lp}) \theta(b_{jp}) \theta(b_{lk}) + \frac{1}{2} \theta(-b_{jp} b_{lk}) \operatorname{sgn}(b_{lp}) \right]. \quad (\text{A36})$$

One sees that though the Arctan function appears in the expression of the integral (A24), it does not enter the expression of $P_{4,jk}$.

Finally, we collect all contributions to $P_{4,jk}$. In $P_{4,jk}^{sym}$ we separate the terms with $p = j$ or $l = k$, which can be combined with the resonance contribution; the rest terms can be combined with the off-resonance contribution. After simplifications, this gives the final expression of the 4th order contribution to the probability P_{jk} for $j < k$:

$$P_{4,jk} = \left(\sum_l^{l < j \text{ or } l > k} \lambda_{jl} \lambda_{lk} \right)^2 + \left(\sum_l^{j < l < k} \lambda_{jl} \lambda_{lk} \right)^2 - \lambda_{jk}^2 \left(\sum_l^{l < k} \lambda_{jl}^2 + 3 \sum_l^{l > k} \lambda_{jl}^2 + \sum_l^{l > j} \lambda_{lk}^2 + 3 \sum_l^{l < j} \lambda_{lk}^2 + 2\lambda_{jk}^2 \right) - 2\lambda_{jk} \left(2 \sum_{l,p}^{p < j < l < k \text{ or } j < p < k < l} - \sum_{l,p}^{j < p < l < k} + \sum_{l,p}^{j < l < k < p, l < j < p < k \text{ or } p < j < k < l} \right) \lambda_{jl} \lambda_{lp} \lambda_{pk}. \quad (\text{A37})$$

Since the matrix P_4 is symmetric, the off-diagonal elements $P_{4,jk}$ with $j > k$ are connected to those in (A37) by

$$P_{4,jk} = P_{4,kj}, \quad \text{for } j > k. \quad (\text{A38})$$

The diagonal elements can then be obtained from the doubly stochastic property of the probability matrix P . We then arrive at the result presented in Section IIIA of the main text.

Note that the probabilities up to 4th order in the couplings can be expressed as polynomials of λ_{jk} with integer coefficients. One may wonder if the same is true for higher order terms of any one-crossing MLZ model, but it turns out that this is not the case. For example, in the one-crossing 5-state LZ model discussed in [2] (the model in Section IVB3 of the main text), one finds from numerics that the higher order terms depend not only on $A_{jk}/\sqrt{|b_{jk}|}$ but also on the ratios of the slope differences b_{jk}/b_{pl} . In fact, in the integral (A24) for the off-resonant case, the Arctan function does depend on the ratios of the slope differences. Although this Arctan function finally does not enter the 4th order terms, it is possible that it does enter higher order terms; there may also be other forms of functions arising from higher-dimensional multiple integrations which also depend on b_{jk}/b_{pl} .

APPENDIX B: INTEGRAL Q IN THE OFF-RESONANT CASE

In this appendix, we present details of calculation of the integral Q in Eq. (A23) in the off-resonant case. For notation simplicity let's write $\alpha = b_{lp}/2$, $\beta = b_{jl}/2$ and $\gamma = b_{pk}/2$, so (A23) becomes

$$Q = \int_0^\infty ds e^{i\alpha s^2} \int_0^s ds_1 e^{i\beta s_1^2} \int_0^s ds_2 e^{i\gamma s_2^2}. \quad (\text{B1})$$

Note the order of the three quantities defined. The resonance condition then reads $\alpha + \beta = 0$ or $\alpha + \gamma = 0$. Note also that we have $\alpha + \beta + \gamma > 0$ since we are considering off-diagonal elements of $W_n(\infty)$ with $j < k$.

As written in (A23), Q can be expressed as an integral of $e^{i\alpha s^2}$ multiplied by two Fresnel integrals with arguments being generally different. An integral of this form cannot be evaluated directly (e.g. using Mathematica). Nevertheless, it can be performed using the parametric integration technique. We first make changes of variables $s = \sqrt{u}$, $s_1 = \sqrt{u_1}$ and $s_2 = \sqrt{u_2}$, so

$$Q = \int_0^\infty du \frac{e^{i\alpha u}}{2\sqrt{u}} \int_0^u du_1 \frac{e^{i\beta u_1}}{2\sqrt{u_1}} \int_0^u du_2 \frac{e^{i\gamma u_2}}{2\sqrt{u_2}}. \quad (\text{B2})$$

We now replace the square roots by using Gaussian integrals of new parameters x , x_1 and x_2 as:

$$\frac{1}{2\sqrt{u}} = \frac{1}{\sqrt{\pi}} \int_0^\infty dx e^{-ux^2}, \quad (\text{B3})$$

and similarly for $\sqrt{u_1}$ and $\sqrt{u_2}$, then

$$Q = \frac{1}{\pi^{\frac{3}{2}}} \int_0^\infty du \int_0^\infty dx e^{(-x^2+i\alpha)u} \int_0^u du_1 \int_0^\infty dx_1 e^{(-x_1^2+i\beta)u_1} \int_0^u du_2 \int_0^\infty dx_2 e^{(-x_2^2+i\gamma)u_2}. \quad (\text{B4})$$

Switching the order of integrations and performing the integrals on u_1 , u_2 , and then u , we get

$$Q = \frac{1}{\pi^{\frac{3}{2}}} \int_0^\infty dx \int_0^\infty dx_1 \int_0^\infty dx_2 \frac{1}{(x_1^2 - i\beta)(x_2^2 - i\gamma)} \times \left[\frac{1}{x^2 - i\alpha} - \frac{1}{x^2 + x_1^2 - i(\alpha + \beta)} - \frac{1}{x^2 + x_2^2 - i(\alpha + \gamma)} + \frac{1}{x^2 + x_1^2 + x_2^2 - i(\alpha + \beta + \gamma)} \right] \equiv Q_1 + Q_2 + Q_3 + Q_4. \quad (\text{B5})$$

Below we evaluate the 4 terms separately. The first term Q_1 separates to three single integrals which can be readily performed:

$$Q_1 = \frac{\pi^{\frac{3}{2}} e^{i\frac{\pi}{4}[\text{sgn}(\alpha) + \text{sgn}(\beta) + \text{sgn}(\gamma)]}}{8\sqrt{|\alpha\beta\gamma|}} = \frac{\pi^{\frac{3}{2}}}{8\sqrt{-i\alpha}\sqrt{-i\beta}\sqrt{-i\gamma}}, \quad (\text{B6})$$

where in obtaining the second equality recall that the branch cut of a square root function is taking to be slightly below the negative real axis, and that α , β and γ are all real and non-zero, so we have

$$\sqrt{-i\alpha} = \sqrt{|\alpha|} e^{-i\frac{\pi}{4}\operatorname{sgn}(\alpha)}, \quad (\text{B7})$$

$$\sqrt{\alpha} = \sqrt{|\alpha|} e^{i\frac{\pi}{4}[1-\operatorname{sgn}(\alpha)]}, \quad (\text{B8})$$

and similarly for β and γ .

The integrals in Q_2 can also be performed directly by first integrating x_2 and x and then x_1 :

$$Q_2 = -\frac{1}{\pi^{\frac{3}{2}}} \frac{\pi}{2\sqrt{-i\gamma}} \int_0^\infty dx_1 \frac{\pi}{2\sqrt{x_1^2 - i(\alpha + \beta)}} \frac{1}{(x_1^2 - i\beta)} = -\frac{\sqrt{\pi}}{4\sqrt{-i\alpha}\sqrt{-i\beta}\sqrt{-i\gamma}} \left[\arctan \frac{\sqrt{-i\alpha}}{\sqrt{-i\beta}\sqrt{1 - i\frac{\alpha+\beta}{x_1^2}}} \right]_{x_1=0}^\infty. \quad (\text{B9})$$

Note that in the last equality the arctan function as an antiderivative should be understood as a multivalued function not restricted to a single branch, and it must change continuously along the integration path from $x_1 = 0$ to $x_1 = \infty$ in order to ensure that its derivative (the integrand) is finite. Thus, in addition to plugging in the principal values of the arctan function at the two limits, one must also examine carefully how its argument changes along the integration path. Whenever this argument crosses a branch cut at $(-i\infty, -i)$ or at $(i, i\infty)$, an additional term $-\pi$ or π should be added to the result from principal values if the crossing is in a counterclockwise or clockwise sense, respectively (viewed from the origin of the complex plane).

With these in mind, we analyze arguments of the arctan function appeared in (B9). When x_1 changes from $x_1 = 0$ to $x_1 = \infty$, the point $\sqrt{|\alpha/\beta|}/\sqrt{1 - i(\alpha + \beta)/x_1^2}$ on the complex plane moves from 0 to $|\alpha/\beta|$ along a path in the upper/lower right half plane for $\alpha + \beta$ being positive/negative, respectively, with its modulus increasing monotonically with x_1 . The phase of $\sqrt{-i\alpha}/\sqrt{-i\beta}$ is $-(\pi/4)[\operatorname{sgn}(\alpha) - \operatorname{sgn}(\beta)]$, whose effect on the path is a global rotation around the origin. Below we discuss different cases:

1. If $|\alpha/\beta| < 1$, the path will never reach a branch cut.
2. If $|\alpha/\beta| > 1$ and $\operatorname{sgn} \alpha = \operatorname{sgn} \beta$, the additional phase is 0, and the path will still not reach a branch cut.
3. If $|\alpha/\beta| > 1$ and $\operatorname{sgn} \alpha \neq \operatorname{sgn} \beta$, then if $\operatorname{sgn} \alpha = -\operatorname{sgn} \beta = 1$ (this ensures $\alpha + \beta > 0$), the path will reach the lower branch cut in the clockwise sense, and this produces an additional term π . On the other hand, if $\operatorname{sgn} \alpha = -\operatorname{sgn} \beta = -1$ (this ensures $\alpha + \beta < 0$), the path will reach the upper branch cut in the counterclockwise sense, but does not cross it. We follow the conventional definition to take the value at a point exactly on a branch cut to be continuous when approached from the counterclockwise direction. So no additional term is added.

In sum, only in the case of $|\alpha/\beta| > 1$ and $\operatorname{sgn} \alpha = -\operatorname{sgn} \beta = 1$ will there be an additional term π . This is equivalent to the requirement that $\beta < 0$ and $\alpha + \beta > 0$. Therefore, we obtain the final result of Q_2 :

$$Q_2 = -\frac{\sqrt{\pi}}{4\sqrt{-i\alpha}\sqrt{-i\beta}\sqrt{-i\gamma}} \left[\theta(-\beta)\theta(\alpha + \beta)\pi + \operatorname{Arctan} \frac{\sqrt{-i\alpha}}{\sqrt{-i\beta}} \right], \quad (\text{B10})$$

where ‘‘Arctan’’ is used to denote the principal value of arctan.

Since the integrand of Q_3 can be obtained from that of Q_2 by exchanging x_1 with x_2 and β with γ , so Q_3 can be obtained from Q_2 simply by switching β and γ in the result of Q_2 :

$$Q_3 = -\frac{\sqrt{\pi}}{4\sqrt{-i\alpha}\sqrt{-i\beta}\sqrt{-i\gamma}} \left[\theta(-\gamma)\theta(\alpha + \gamma)\pi + \operatorname{Arctan} \frac{\sqrt{-i\alpha}}{\sqrt{-i\gamma}} \right], \quad (\text{B11})$$

Finally we evaluate Q_4 , which is the most complicated. Performing first the integration on x gives:

$$Q_4 = \frac{1}{\pi^{\frac{3}{2}}} \int_0^\infty dx_1 \int_0^\infty dx_2 \frac{1}{(x_1^2 - i\beta)(x_2^2 - i\gamma)} \frac{\pi}{2\sqrt{x_1^2 + x_2^2 - i(\alpha + \beta + \gamma)}}. \quad (\text{B12})$$

Introduce polar coordinates $x_1 = r \cos \varphi$ and $x_2 = r \sin \varphi$, Q_4 is rewritten as

$$Q_4 = \frac{1}{\pi^{\frac{3}{2}}} \int_0^\infty dr r \frac{\pi}{2\sqrt{r^2 - i(\alpha + \beta + \gamma)}} I_\varphi, \quad (\text{B13})$$

where we denoted the angular integral as

$$I_\varphi \equiv \int_0^{\frac{\pi}{2}} d\varphi \frac{1}{(r^2 \cos^2 \varphi - i\beta)(r^2 \sin^2 \varphi - i\gamma)}. \quad (\text{B14})$$

I_φ can be performed by contour integration. Using symmetry to extend the integral region and changing variable to $\theta = 2\varphi$, we get

$$I_\varphi = \frac{1}{4} \int_0^{2\pi} d\theta \frac{1}{\left[\frac{r^2}{2}(1 + \cos \theta) - i\beta\right] \left[\frac{r^2}{2}(1 - \cos \theta) - i\gamma\right]}. \quad (\text{B15})$$

A transformation $z = e^{i\theta}$ then recasts the integral as one along a unit circle of an complex variable z :

$$I_\varphi = \frac{1}{4} \oint_{|z|=1} \frac{dz}{iz} \frac{1}{\left[\frac{r^2}{2}(1 + \frac{z^2+1}{2z}) - i\beta\right] \left[\frac{r^2}{2}(1 - \frac{z^2+1}{2z}) - i\gamma\right]}. \quad (\text{B16})$$

Application of the residue theorem then gives:

$$I_\varphi = \frac{\pi}{2} \sum_{|z|<1} \text{res} \frac{1}{z \left[\frac{r^2}{2}(1 + \frac{z^2+1}{2z}) - i\beta\right] \left[\frac{r^2}{2}(1 - \frac{z^2+1}{2z}) - i\gamma\right]}, \quad (\text{B17})$$

where the sum is over all singular points inside the unit circle. The singular points are located at the roots of two equations:

$$z^2 + 2(1 - i\frac{2\beta}{r^2})z + 1 = 0, \quad (\text{B18})$$

$$z^2 - 2(1 - i\frac{2\gamma}{r^2})z + 1 = 0, \quad (\text{B19})$$

which are

$$z_{1,2} = -1 + i\frac{2\beta}{r^2} \pm \sqrt{\left(1 - i\frac{2\beta}{r^2}\right)^2 - 1}, \quad (\text{B20})$$

$$z_{3,4} = 1 - i\frac{2\gamma}{r^2} \pm \sqrt{\left(1 - i\frac{2\gamma}{r^2}\right)^2 - 1}. \quad (\text{B21})$$

Only the two roots z_1 and z_4 are in the unit circle and contribute to the sum of residues. Calculating out these two residues, we obtain

$$I_\varphi = \frac{\pi}{2[r^2 - i(\beta + \gamma)]} \left[\frac{1}{\sqrt{-\beta(\beta + ir^2)}} + \frac{1}{\sqrt{-\gamma(\gamma + ir^2)}} \right]. \quad (\text{B22})$$

Plugging into (B13) and changing variable to $y = r^2$, we get Q_4 expressed as a single integral:

$$Q_4 = \frac{\sqrt{\pi}}{8} \int_0^\infty dy \frac{1}{\sqrt{y - i(\alpha + \beta + \gamma)}} \frac{1}{y - i(\beta + \gamma)} \left[\frac{1}{\sqrt{-\beta(\beta + iy)}} + \frac{1}{\sqrt{-\gamma(\gamma + iy)}} \right]. \quad (\text{B23})$$

The two terms in the integrand are symmetric in β and γ . For the first term, direct integration gives:

$$I_y \equiv \int_0^\infty dy \frac{1}{\sqrt{y - i(\alpha + \beta + \gamma)}} \frac{1}{y - i(\beta + \gamma)} \frac{1}{\sqrt{-\beta(\beta + iy)}} = \frac{2}{\sqrt{-i\alpha}\sqrt{-i\beta}\sqrt{-i\gamma}} \left[\arctan \frac{\sqrt{-i\alpha}\sqrt{y - i\beta}}{\sqrt{-i\gamma}\sqrt{y - i(\alpha + \beta + \gamma)}} \right]_{y=0}^\infty, \quad (\text{B24})$$

where we used the fact that since β is real and y is positive, $\sqrt{-\beta(\beta + iy)} = \sqrt{-i\beta}\sqrt{y - i\beta}$ always holds. The second term in (B23) can be obtained from I_y by switching β and γ . We thus obtain Q_4 :

$$Q_4 = \frac{\sqrt{\pi}}{8} [I_y + (\beta \leftrightarrow \gamma)] = \frac{\sqrt{\pi}}{4\sqrt{-i\alpha}\sqrt{-i\beta}\sqrt{-i\gamma}} \left[\arctan \frac{\sqrt{-i\alpha}\sqrt{y - i\beta}}{\sqrt{-i\gamma}\sqrt{y - i(\alpha + \beta + \gamma)}} + \arctan \frac{\sqrt{-i\alpha}\sqrt{y - i\gamma}}{\sqrt{-i\beta}\sqrt{y - i(\alpha + \beta + \gamma)}} \right]_{y=0}^\infty. \quad (\text{B25})$$

Again, the arguments of the arctan functions need careful treatment. Instead of treating directly the arctan function in Q_4 , it turns out to be more convenient to first combine the results of Q_2 , Q_3 and Q_4 for in terms of the antiderivatives:

$$Q_2 + Q_3 + Q_4 = \frac{\sqrt{\pi}}{4\sqrt{-i\alpha}\sqrt{-i\beta}\sqrt{-i\gamma}} \times \left[-\arctan \frac{\sqrt{-i\alpha}}{\sqrt{-i\beta}\sqrt{1-i\frac{\alpha+\beta}{y}}} - \arctan \frac{\sqrt{-i\alpha}}{\sqrt{-i\gamma}\sqrt{1-i\frac{\alpha+\gamma}{y}}} + \arctan \frac{\sqrt{-i\alpha}\sqrt{y-i\beta}}{\sqrt{-i\gamma}\sqrt{y-i(\alpha+\beta+\gamma)}} \right. \\ \left. + \arctan \frac{\sqrt{-i\alpha}\sqrt{y-i\gamma}}{\sqrt{-i\beta}\sqrt{y-i(\alpha+\beta+\gamma)}} \right]_{y=0}^{\infty} \quad (B26)$$

where we have changed the dummy integration variables in Q_2 and Q_3 from x_1^2 and x_2^2 to y . The second/third term can be obtained from the first/fourth term respectively by exchanging β and γ , so it suffices to consider the first and fourth terms. We also reverse the two limits in the fourth term, so

$$Q_2 + Q_3 + Q_4 = -\frac{\sqrt{\pi}}{4\sqrt{-i\alpha}\sqrt{-i\beta}\sqrt{-i\gamma}} \times \left\{ \left[\arctan \frac{\sqrt{-i\alpha}}{\sqrt{-i\beta}\sqrt{1-i\frac{\alpha+\beta}{y}}} \right]_{y=0}^{\infty} + \left[\arctan \frac{\sqrt{-i\alpha}\sqrt{y-i\gamma}}{\sqrt{-i\beta}\sqrt{y-i(\alpha+\beta+\gamma)}} \right]_{y=\infty}^0 \right\} + (\beta \leftrightarrow \gamma). \quad (B27)$$

We now need to analyze at which condition will the path make a finite contribution to the result from principal values. In (B27) the argument of the first arctan function moves from 0 at $y = 0$ to $\sqrt{-i\alpha}/\sqrt{-i\beta}$ at $y = \infty$, and the argument of the second arctan function moves from $\sqrt{-i\alpha}/\sqrt{-i\beta}$ at $y = \infty$ to $\sqrt{-i\alpha}\sqrt{-i\gamma}/[\sqrt{-i\beta}\sqrt{-i(\alpha+\beta+\gamma)}]$ at $y = 0$. So the two paths are connected to a single one. Plotting at different choices of α , β and γ shows that such a connected path always lies in a single quadrant of the complex plane, so it can never cross a branch cut. But it can end exactly on a branch cut. This can only happen when the final point's modulus satisfies $|(\alpha\gamma)/[\beta(\alpha+\beta+\gamma)]| > 1$ and its phase satisfies $\arg[\sqrt{-i\alpha}\sqrt{-i\gamma}/(\sqrt{-i\beta}\sqrt{-i(\alpha+\beta+\gamma)})] = \pi[-\text{sgn}(\alpha) + \text{sgn}(\beta) - \text{sgn}(\gamma) + \text{sgn}(\alpha+\beta+\gamma)]/4 = \pm\pi/2$, where the upper/lower signs correspond to the upper and lower branch cuts, respectively. Further, according to the definition of values on a branch cut, in order to produce a finite contribution to the result, the path must approach the branch cut in the clockwise sense. This can only take place when the path from 0 to $\sqrt{-i\alpha}/\sqrt{-i\beta}$ is in the second/fourth quadrant if the path ends at the upper/lower branch cut, respectively. Looking at the value of the argument at $y = 0^+$ gives the condition $\pi[-\text{sgn}(\alpha) + \text{sgn}(\beta) + \text{sgn}(\alpha+\beta)]/4 = 3\pi/4$ or $-\pi/4$. Setting it to $3\pi/4$ gives $\alpha < 0$ and $\alpha + \beta > 0$, and setting it to $-\pi/4$ gives $\alpha < 0$ and $\beta < 0$, or $\beta < 0$ and $\alpha + \beta > 0$. Thus, there are two cases for the signs. Case 1 is (recall that $\alpha + \beta + \gamma > 0$)

$$\begin{aligned} -\text{sgn}(\alpha) + \text{sgn}(\beta) - \text{sgn}(\gamma) &= 1, \\ -\text{sgn}(\alpha) + \text{sgn}(\beta) + \text{sgn}(\alpha + \beta) &= 3, \end{aligned} \quad (B28)$$

Case 2 is

$$\begin{aligned} -\text{sgn}(\alpha) + \text{sgn}(\beta) - \text{sgn}(\gamma) &= -3, \\ -\text{sgn}(\alpha) + \text{sgn}(\beta) + \text{sgn}(\alpha + \beta) &= -1. \end{aligned} \quad (B29)$$

Cases 1 gives: $\alpha < 0$, $\beta > 0$, $\gamma > 0$, and $\alpha + \beta > 0$. Cases 2 gives: $\alpha > 0$, $\beta < 0$, $\gamma > 0$, and $\alpha + \beta > 0$. But note that for case 1, one always has $|\alpha| < |\beta|$ and $|\gamma| < |\alpha + \beta + \gamma|$, so $|(\alpha\gamma)/[\beta(\alpha + \beta + \gamma)]| > 1$ can never be satisfied, so case 1 is not possible. For case 2, one has $|\alpha| > |\beta|$ and $|\gamma| < |\alpha + \beta + \gamma|$, and $|(\alpha\gamma)/[\beta(\alpha + \beta + \gamma)]| > 1$ reduces to $-\alpha\gamma/[\beta(\alpha + \beta + \gamma)] > 1$, or $(\alpha + \beta)(\beta + \gamma) > 0$. This together with $\alpha + \beta > 0$ gives $\beta + \gamma > 0$. In sum, only in the case of $\beta < 0$, $\alpha + \beta > 0$ and $\beta + \gamma > 0$ will there be an additional term π added to the result of the first two arctan functions in (B27). Thus,

$$\begin{aligned} & \left[\arctan \frac{\sqrt{-i\alpha}}{\sqrt{-i\beta}\sqrt{1-i\frac{\alpha+\beta}{y}}} \right]_{y=0}^{\infty} + \left[\arctan \frac{\sqrt{-i\alpha}\sqrt{y-i\gamma}}{\sqrt{-i\beta}\sqrt{y-i(\alpha+\beta+\gamma)}} \right]_{y=\infty}^0 \\ &= \theta(-\beta)\theta(\alpha+\beta)\theta(\beta+\gamma)\pi + \text{Arctan} \frac{\sqrt{-i\alpha}\sqrt{-i\gamma}}{\sqrt{-i\beta}\sqrt{-i(\alpha+\beta+\gamma)}}. \end{aligned} \quad (B30)$$

The term with step functions affects only those cases at which the argument of the Arctan function lies on the lower branch cut and satisfy $\beta < 0$, $\alpha + \beta > 0$ and $\beta + \gamma > 0$. Note an Arctan function has a real part within $[-\pi/2, \pi/2]$, and when its argument is on the lower branch cut its real part is $-\pi/2$. Thus, the result of (B30) still has a real part within $[-\pi/2, \pi/2]$. The conditions for which a π needs to be added to the “ $(\beta \leftrightarrow \gamma)$ ” terms can be obtained directly by switching β with γ . Finally we get:

$$Q_2 + Q_3 + Q_4 = -\frac{\sqrt{\pi}}{4\sqrt{-i\alpha}\sqrt{-i\beta}\sqrt{-i\gamma}} \left[\theta(-\beta)\theta(\alpha + \beta)\theta(\beta + \gamma)\pi + \text{Arctan} \frac{\sqrt{-i\alpha}\sqrt{-i\gamma}}{\sqrt{-i\beta}\sqrt{-i(\alpha + \beta + \gamma)}} \right] + (\beta \leftrightarrow \gamma). \quad (\text{B31})$$

The two arctan functions can be combined by using

$$\text{Arctan}(z_1) + \text{Arctan}(z_2) = \text{Arctan} \frac{z_1 + z_2}{1 - z_1 z_2} + M\pi, \quad (\text{B32})$$

where the additional $M\pi$ term with M an integer is needed to connect values at different branches. Here we have $z_1 = \sqrt{-i\alpha}\sqrt{-i\beta}/[\sqrt{-i\gamma}\sqrt{-i(\alpha + \beta + \gamma)}]$ and $z_2 = \sqrt{-i\alpha}\sqrt{-i\gamma}/[\sqrt{-i\beta}\sqrt{-i(\alpha + \beta + \gamma)}]$, and $(z_1 + z_2)/(1 - z_1 z_2)$ can be reduced to a simple form:

$$\frac{(z_1 + z_2)}{1 - z_1 z_2} = \frac{\sqrt{-i\alpha}\sqrt{-i(\alpha + \beta + \gamma)}}{\sqrt{-i\beta}\sqrt{-i\gamma}}. \quad (\text{B33})$$

The integer M can be determined by calculating out numerical values at different choices α , β and γ . It turns out that $M = 1$ when $\alpha + \beta > 0$, $\alpha + \gamma > 0$ and $\beta + \gamma < 0$ or when $\alpha + \beta < 0$ and $\alpha + \gamma < 0$ are satisfied, and $M = 0$ otherwise. Thus,

$$M = \theta(\alpha + \beta)\theta(\alpha + \gamma)\theta(-\beta - \gamma) + \theta(-\alpha - \beta)\theta(-\alpha - \gamma). \quad (\text{B34})$$

This contribution from $M\pi$ can be combined with the term with step functions in (B31), and we arrive at

$$Q_2 + Q_3 + Q_4 = -\frac{\sqrt{\pi}}{4\sqrt{-i\alpha}\sqrt{-i\beta}\sqrt{-i\gamma}} \times \left\{ \{\theta[(\alpha + \beta)(\alpha + \gamma)] - \theta(\beta)\theta(\gamma)\theta(\alpha + \beta)\theta(\alpha + \gamma)\}\pi + \text{Arctan} \frac{\sqrt{-i\alpha}\sqrt{-i(\alpha + \beta + \gamma)}}{\sqrt{-i\beta}\sqrt{-i\gamma}} \right\}, \quad (\text{B35})$$

which can further be written as

$$Q_2 + Q_3 + Q_4 = -\frac{\sqrt{\pi}}{4\sqrt{-i\alpha}\sqrt{-i\beta}\sqrt{-i\gamma}} \left\{ \left[\frac{1}{2} - \theta(-\alpha)\theta(\alpha + \beta)\theta(\alpha + \gamma) \right] \pi - \text{Arctan} \frac{\sqrt{-i\beta}\sqrt{-i\gamma}}{\sqrt{-i\alpha}\sqrt{-i(\alpha + \beta + \gamma)}} \right\}. \quad (\text{B36})$$

Combining with Q_1 , finally we obtain Q :

$$Q = \frac{\sqrt{\pi}}{4\sqrt{-i\alpha}\sqrt{-i\beta}\sqrt{-i\gamma}} \left[\theta(-\alpha)\theta(\alpha + \beta)\theta(\alpha + \gamma)\pi + \text{Arctan} \frac{\sqrt{-i\beta}\sqrt{-i\gamma}}{\sqrt{-i\alpha}\sqrt{-i(\alpha + \beta + \gamma)}} \right]. \quad (\text{B37})$$

Writing α , β and γ back to the slopes, we get (A24).

We checked at different sets of values of α , β and γ that the expression (B37) agrees with results of numerical integration of (B1). But the Arctan function in (B37) diverges at special choices of α , β and γ when its argument happens to be at the branch points $\pm i$, and (B37) does not apply in this special case. This takes place when

$$\left[\frac{\sqrt{-i\beta}\sqrt{-i\gamma}}{\sqrt{-i\alpha}\sqrt{-i(\alpha + \beta + \gamma)}} \right]^2 = \frac{\beta\gamma}{\alpha(\alpha + \beta + \gamma)} = -1, \quad (\text{B38})$$

or

$$(\alpha + \beta)(\alpha + \gamma) = 0. \quad (\text{B39})$$

Therefore, (B37) is not applicable whenever any of the two conditions

$$\alpha + \beta = 0, \quad (\text{B40})$$

$$\alpha + \gamma = 0, \quad (\text{B41})$$

are satisfied. Writing them in terms of the slopes, we arrive at the resonance condition discussed in the main text.

APPENDIX C: 4-STATE LZ MODEL WITH ALL-TO-ALL COUPLINGS

In this appendix, we present perturbative results for the most general one-crossing 4-state LZ model, with a Hamiltonian:

$$H = \begin{pmatrix} b_1 t & A_{12} & A_{13} & A_{14} \\ A_{12} & b_2 t & A_{23} & A_{24} \\ A_{13} & A_{23} & b_3 t & A_{34} \\ A_{14} & A_{24} & A_{34} & b_4 t \end{pmatrix}, \quad (\text{C1})$$

where $b_1 > b_2 > b_3 > b_4$. We obtain:

$$P_{12} = 2\lambda_{12}^2 - 2\lambda_{12}(\lambda_{13}\lambda_{23} + \lambda_{14}\lambda_{24}) + (\lambda_{13}\lambda_{23} + \lambda_{14}\lambda_{24})^2 - \lambda_{12}^2[3(\lambda_{13}^2 + \lambda_{14}^2) + \lambda_{23}^2 + \lambda_{24}^2 + 2\lambda_{12}^2] + O(g^5), \quad (\text{C2})$$

$$P_{13} = 2\lambda_{13}^2 + 2\lambda_{13}(\lambda_{12}\lambda_{23} - \lambda_{14}\lambda_{34}) + \lambda_{12}^2\lambda_{23}^2 + \lambda_{14}^2\lambda_{34}^2 - \lambda_{13}^2(\lambda_{12}^2 + 3\lambda_{14}^2 + \lambda_{23}^2 + \lambda_{34}^2 + 2\lambda_{13}^2) - 2\lambda_{13}(2\lambda_{14}\lambda_{24}\lambda_{23} + \lambda_{12}\lambda_{24}\lambda_{34}) + O(g^5), \quad (\text{C3})$$

$$P_{14} = 2\lambda_{14}^2 + 2\lambda_{14}(\lambda_{12}\lambda_{24} + \lambda_{13}\lambda_{34}) + (\lambda_{12}\lambda_{24} + \lambda_{13}\lambda_{34})^2 - \lambda_{14}^2(\lambda_{12}^2 + \lambda_{13}^2 + \lambda_{24}^2 + \lambda_{34}^2 + 2\lambda_{14}^2) + 2\lambda_{14}\lambda_{13}\lambda_{23}\lambda_{24} + O(g^5), \quad (\text{C4})$$

$$P_{23} = 2\lambda_{23}^2 - 2\lambda_{23}(\lambda_{12}\lambda_{13} + \lambda_{24}\lambda_{34}) + (\lambda_{12}\lambda_{13} + \lambda_{24}\lambda_{34})^2 - \lambda_{23}^2(\lambda_{12}^2 + 3\lambda_{24}^2 + \lambda_{34}^2 + 3\lambda_{13}^2 + 2\lambda_{23}^2) - 2\lambda_{23}\lambda_{24}\lambda_{14}\lambda_{13} + O(g^5), \quad (\text{C5})$$

$$P_{11} = 1 - 2(\lambda_{12}^2 + \lambda_{13}^2 + \lambda_{14}^2) + 2(\lambda_{12}^2 + \lambda_{13}^2 + \lambda_{14}^2)^2 + O(g^6), \quad (\text{C6})$$

$$P_{22} = 1 - 2(\lambda_{12}^2 + \lambda_{23}^2 + \lambda_{24}^2) + 2\lambda_{12}^4 + 2\lambda_{12}^2(\lambda_{13}^2 + \lambda_{14}^2 + \lambda_{23}^2 + \lambda_{24}^2) + \lambda_{23}^2(2\lambda_{13}^2 + 3\lambda_{24}^2 + 2\lambda_{23}^2) + \lambda_{24}^2(2\lambda_{14}^2 + \lambda_{23}^2) + 2\lambda_{24}^4 + 4\lambda_{13}\lambda_{14}\lambda_{23}\lambda_{24} + O(g^6). \quad (\text{C7})$$

Again, other P_{jk} with $j \leq k$ are connected to these explicitly written out ones by switches of indices $1 \leftrightarrow 4$ and $2 \leftrightarrow 3$ everywhere, and P_{jk} with $j > k$ can be obtained by changing the signs of the 3rd order terms in P_{kj} . We do not perform numerical checks for this model, but note that P_{11} in (C6) agrees with the exact result from the BE formula.

[1] M. Abramowitz and I. Stegun, *Handbook of Mathematical Functions: With Formulas, Graphs, and Mathematical Tables* (Dover Publications, 1965).
[2] R. Hu, F. Li, and C. Sun, Solution to a class of multistate Landau-Zener model beyond integrability conditions, *Phys. Scr.* **99**, 065226 (2024).